First posted online on 16 August 2018 as 10.1242/dmm.035634
Access the most recent version at http://dmm.biologists.org/lookup/doi/10.1242/dmm.035634

Correction of cognitive deficits in mouse models of Down syndrome by a pharmacological inhibitor of DYRK1A

Thu Lan **NGUYEN**[1,2,3,4,5], Arnaud **DUCHON**[1,2,3,4], Antigoni **MANOUSOPOULOU**[6], Nadège **LOAËC**[5], Benoît **VILLIERS**[5], Guillaume **PANI**[1,2,3,4], Meltem **KARATAS**[7,8], Anna E **MECHLING**[8], Laura-Adela **HARSAN**[7,8], Emmanuelle **LIMANTON**[9], Jean-Pierre **BAZUREAU**[9], François **CARREAUX**[9], Spiros D. **GARBIS**[6]**, Laurent **MEIJER**[5]** and Yann **HERAULT**[1,2,3,4]**

1. Institut de Génétique et de Biologie Moléculaire et Cellulaire, Department of Translational Medicine and Neurogenetics, Illkirch, France.
2. Centre National de la Recherche Scientifique, UMR7104, Illkirch, France.
3. Institut National de la Santé et de la Recherche Médicale, U964, Illkirch, France.
4. Université de Strasbourg, Illkirch, France.
5. ManRos Therapeutics, Perharidy Research Center, 29680 Roscoff, Bretagne, France.
6. Faculty of Medicine / Cancer Sciences & Clinical and Experimental Medicine, University of Southampton, Center for Proteomic Research, Life Sciences Building 85, Highfield, Southampton, SO17 1BJ, UK.
7. Laboratory of Engineering, Informatics and Imaging (ICube), Integrative multimodal imaging in healthcare (IMIS), *UMR 7357*, and University Hospital Strasbourg, Department of Biophysics and Nuclear Medicine, University of Strasbourg.
8. Department of Radiology, Medical Physics, Medical Center – University of Freiburg, Breisacher Strasse 60a, 79106 Freiburg, Germany
9. Université de Rennes 1, Laboratoire Sciences Chimiques de Rennes, UMR CNRS 6226, Groupe Ingénierie Chimique & Molécules pour le Vivant (ICMV), Bât. 10A, Campus de Beaulieu, Avenue du Général Leclerc, CS 74205, 35042 Rennes cedex, France.

** Correspondence should be addressed to:

Phosphoproteomics: S.D. Garbis (<S.D.Garbis@soton.ac.uk>)

Kinase inhibitors: L. Meijer (<meijer@manros-therapeutics.com>)

Down syndrome: Y. Hérault (<herault@igbmc.fr>)

Key words: DYRK1A, Kinase inhibitor, Leucettine, Down syndrome, Synapsin.

ABBREVIATIONS

ACA, rostral and medial anterior cingulate cortex; **ACC,** anterior cingulate cortex; **AD**, Alzheimer's disease; **AMBA**, Allen mouse brain atlas; **BAC**, bacterial artificial chromosome; **BBB**, blood brain barrier; **CAMK2A**, calmodulin-dependent kinase 2A; **CNR1**, cannabinoid receptor 1; **CDK**, cyclin-dependent kinase; **CLK**, cdc2-like kinase; **Co-IP**, co-immunoprecipitation; **DG**, dentate gyrus; **DMN**, default mode network; **DMSO**, dimethylsulfoxide; **DS**, Down syndrome; **DYRK**, dual specificity, tyrosine phosphorylation regulated kinase; **ECL**, enhanced chemiluminescence reaction; **EGCG**, epigallocatechin gallate; **ES**, enrichment score; **FC**, functional connectivity; **GluN2A**, N-methyl-D-aspartate receptor subunit 2A; **GLUR1**, AMPA-selective glutamate receptor 1; **GSK-3**, glycogen synthase kinase-3; **HF**, hippocampal formation; **HSA21**, human chromosome 21; **IP**, immunoprecipitate; **LTD**, long term depression; **LTP**, long term potentiation; **MRD7**, mental retardation, autosomal dominant 7; **MWM**, Morris water maze; **NFATc4**, Nuclear factor of activated T-cells cF4; **NLS**, nuclear localization signal; **NOR**, novel object recognition; **PAL**, pallidum; **PCLO**, Piccolo; **PFC**, prefrontal cortex; **PSD**, postsynaptic density; **PSD95**, postsynaptic density protein 95; **PTLp**, posterior parietal association areas; **RPLPO**, ribosomal protein, large, P0; **rsfMRI**, resting state functional magnetic resonance imaging; **RSP**, retrosplenial; **SDS-PAGE**, sodium dodecyl sulfate, polyacrylamide gel electrophoresis; SC, superior colliculus; **SV**, synaptic vesicle; **SYN1**, synapsin 1; **SYNJ1**, synaptojanin 1; **TEa**, temporal association areas; **TH**, thalamus; **VIS**, visual areas;**WB**, Western blotting; **wt**, wild-type; **YAC**, yeast artificial chromosome.

ABSTRACT

Growing evidence support the implication of DYRK1A in the development of cognitive deficits seen in Down syndrome (DS) and Alzheimer's disease (AD). We here demonstrate that pharmacological inhibition of brain DYRK1A is able to correct recognition memory deficits in three DS mouse models with increasing genetic complexity (Tg(*Dyrk1a*), Ts65Dn, Dp1Yey), all expressing an extra copy of *Dyrk1a*. Overexpressed DYRK1A accumulates in the cytoplasm and at the synapse. Treatment of the three DS models with the pharmacological DYRK1A inhibitor Leucettine L41 leads to normalization of DYRK1A activity and corrects the novel object cognitive impairment observed in these models. Brain functional magnetic resonance imaging reveals that this cognitive improvement is paralleled by functional connectivity remodeling of core brain areas involved in learning/memory processes. The impact of *Dyrk1a* trisomy and L41 treatment on brain phosphoproteins was investigated by a phosphoproteomics approach, revealing the implication of synaptic (synapsin I) and cytoskeletal components involved in synaptic response and axonal organization. These results encourage the development of DYRK1A inhibitors as drug candidates to treat cognitive deficits associated with DS and AD.

INTRODUCTION

Down Syndrome (DS) results from the trisomy of human chromosome 21 (HSA21). It is still the most frequent intellectual disability, affecting 1 newborn per 700 births. Among the most common DS features are hypotonia, dysmorphic features and intellectual disability (Sureshbabu et al. 2011; Morris, Vaughan, and Vaccaro 1982). Although children with DS show good socialization skills, encompassing social relations, friendship and leisure activities, they exhibit difficulties in communication abilities, i.e. the daily use of receptive, expressive and written language (Marchal et al. 2016). They experience troubles in daily life skills, such as self-caring, eating, toileting, dressing, behaving safely and conceptualizing time and money. Improving the intellectual quotient of DS people would allow them to reach more independence, better vigilance and globally improve their quality of life.

Among candidate genes explaining intellectual disabilities in DS people, the dual specificity tyrosine-phosphorylation regulated kinase 1A, *DYRK1A*, is located in the DS chromosome 21 critical region (Walte et al., 2013; Duchon and Herault 2016). It encodes a serine/threonine kinase which has numerous substrates. Two nuclear localization signals (NLS) confer a nuclear activity to this kinase (Alvarez et al. 2007), through interactions with transcription factors including GLI1 (Mao et al. 2002), RNA POL II (DiVona et al. 2015) or splicing factors like cyclin L2 (Graaf et al. 2004). In the cytoplasm, DYRK1A phosphorylates cytoskeletal substrates such as b-Tubulin, MAP1A or MAP1B (Ori-McKenney et al. 2016; Murakami et al. 2012; Scales et al. 2009). DYRK1A plays a role in cell cycle regulation by phosphorylating the cyclin-dependent kinase (CDK) inhibitor KIP1 in cultured hippocampal neurons and in embryonic mouse brain (Soppa et al. 2014) and LIN52 *in vitro* (Litovchick et al. 2011). Through its 'priming' activity for GSK-3β (glycogen synthase kinase 3β) dependent phosphorylation DYRK1A regulates the nuclear/cytoplasmic localization of the transcription factor NFATc4 (Arron et al. 2006). At the synaptic level DYRK1A binds to GLUN2A (N-methyl-D-aspartate receptor subunit 2A) and SYNJ1 (synaptojanin 1) (Chen et al. 2014; Grau et al. 2014) and phosphorylates Amphyphysin 1 (Murakami et al. 2012) and GLUN2A (Grau et al. 2014). These are examples of different biological brain functions controlled by DYRK1A which are probably dysregulated when DYRK1A is overexpressed in DS, leading to cognitive impairments.

Several mouse models overexpressing DYRK1A have been described. The first one, Tg(CEPHY152F7)12Hgc, carries a single copy of a yeast artificial chromosome (YAC) containing a 570 kb-fragment of human DNA encompassing *TTC3*, *DYRK1A* and *KCNJ6*. This model shows no strong defect in spatial learning and memory but displays less crossing

of the site where the platform was during the probe test in the Morris water maze (MWM) (D. J. Smith et al. 1997). Another model, Tg(MT1A-*Dyrk1a*)#Xest (# =9 or 33), was produced by expressing the *Dyrk1a* rat cDNA under the control of the metallothionein 1a exogenous promoter (Altafaj et al. 2001). These mice demonstrated impairments in neuromotor development and hyperactivity evaluated in the Treadmill performance and Rotarod tests (Martínez de Lagrán et al. 2004). They also display defects in visuo-spatial learning and memory in the MWM test (Martínez de Lagrán et al. 2004; Pons-Espinal, Martinez de Lagran, and Dierssen 2013) as well as in recognition memory revealed in the novel object recognition (NOR) task (Torre et al. 2014a). A third model, Tg(*DYRK1A*)36Wjs, was generated using a bacterial artificial chromosome (BAC) containing the human *DYRK1A* gene. *DYRK1A* triplication leads to alterations in synaptic transmission with an increase in long term potentiation (LTP) and a decrease in long term depression (LTD). The transgenic mice are also deficient in the MWM task, suggesting spatial learning and memorization disabilities (Ahn et al. 2006). Although the human YAC and BAC transgenic mice exhibit features similar to those seen in DS patients, they carry an extra copy of human/rat *DYRK1A* gene which could lead to biased phenotypes as optimal expression and functionality of the human/rat protein cannot be ensured in a mouse background. Therefore a BAC transgenic model with the entire *Dyrk1a* murine gene, Tg(*Dyrk1a*)189N3Yah (hereafter Tg(*Dyrk1a*)), was created (Guedj et al. 2012). This model shows alterations in short term memory in the Y-maze task, and in spatial memory in the MWM test (Souchet et al. 2014). Deficits in cortical synaptic plasticity was also observed (Thomazeau et al. 2014). Comparable impairments were seen in the Ts(17^{16})65Dn (hereafter Ts65Dn), a mouse model trisomic for almost 13,4 Mb homologous to HSA21 and containing *DYRK1A* (Reeves et al. 1995). Spatial memory, especially reversal learning reflecting cognitive flexibility, was altered in the Water T-maze test and in the reversal version of the MWM (Olmos-Serrano et al. 2016). Although the Ts65Dn model has been widely used to study DS features, it carries a triplication of genes located in a subcentromeric region of MMU17 which are not syntenic to any HSA21 genes (Duchon et al. 2011). A complete DS model, Dp1Yey, was thus produced, it is trisomic for 22.9 Mb, spanning the entire HSA21 region on MMU16 (Li et al. 2007). Dp1Yey mice are less performing than control mice in the MWM task and display context-associated learning deficits in the Fear conditioning test (Yu et al. 2010).

Reducing DYRK1A overdosage leads to correction of several DS traits, demonstrating the major implication of this kinase in DS. Indeed, normalization of DYRK1A expression attenuates spatial learning as well as associative memory defects and rescues LTP in the Ts65Dn model (García-Cerro et al. 2014; Altafaj et al. 2013). In addition, reversal to two DYRK1A copies in Dp1Yey mice enhances working and associative learning performance assessed in the T-maze and contextual Fear-conditioning tests, respectively (Jiang et al. 2015). Furthermore, epigallocatechin gallate (EGCG), a natural polyphenol found in coffee, cocoa and green tea, reported to inhibit DYRK1A, restores intellectual capacities of trisomic mice (Guedj et al. 2009; Torre et al. 2014b). EGCG has undergone a phase 2 clinical trial (Torre et al. 2016). However EGCG interacts with the cannabinoid receptor 1 (CNR1) (Korte et al. 2010). This receptor modulates the release of neurotransmitters in various brain areas, such as prefrontal cortex and hippocampus, thereby controlling memory, cognition processes and mood. Interaction with CNR1 might thus affect memory, cognition and pain perception, leading to psychiatric disorders (Freund, Katona, and Piomelli 2003; Wilson and Nicoll 2002). This compromised the therapeutic use of EGCG. Furthermore, DYRK1A (IC_{50}: 0.33 µM) is less sensitive to EGCG than vimentin (IC_{50}: 0.003 µM) and the laminin receptor (IC_{50}: 0.04 µM) (Khan et al. 2006; Yang et al. 2009). Cognitive restoration in trisomic mice by EGCG may thus be due to inhibition of targets other than DYRK1A. Consequently more recent pharmacological inhibitors have started to emerge (Kim et al., 2016; Nakano-Kobayashi et al., 2017; Nguyen et al., 2017). Nevertheless, all available results clearly demonstrate the implication of DYRK1A in DS intellectual deficiencies and the beneficial effects of its inhibition on the correction of cognitive deficits.

DYRK1A has become a major screening target for the development of selective and potent pharmacological inhibitors (reviews in Smith et al., 2012; Stotani et al., 2016; Nguyen et al., 2017). We here investigated the effects of a relatively selective DYRK1A inhibitor, Leucettine 41 (hereafter L41) in three different trisomic mouse models with increasing genetic complexity, Tg(*Dyrk1a*), Ts65Dn and Dp1Yey. Leucettines are derived from the marine sponge alkaloid Leucettamine B (Debdab et al., 2011; Tahtouh et al. 2012). The chemically synthesized L41 displays a high selectivity for DYRK1A but also DYRK1B, DYRK2 and some CLKs (Cdc2-like kinases) (Figure 1). It acts by competing with ATP binding to the kinase catalytic site. We here establish a proof of concept that pharmacological inhibition of brain DYRK1A is able to correct NOR cognitive impairment in three DS models with increasing genetic complexity. We show via brain functional magnetic resonance imaging (fMRI), in Dp1Yey, the most complete mouse model of DS, that such cognitive

improvement is paralleled by significant functional connectivity remodeling of core brain areas involved in learning and memory processes. Furthermore, phosphoproteomic analyses in the Tg(*Dyrk1a*) model unraveled brain DYRK1A targets which phosphorylation increases with DYRK1A overdosage and decreases following L41 treatment. These novel substrates, such as synapsin I, also found in the phosphoproteomic analyses of Ts65Dn, the most used DS model, bring new insight on the role of DYRK1A and allow us to propose some dysregulated biological processes related to axonal organization and synaptic response which are responsible for cognitive deficits associated with DS.

RESULTS

Leucettines restore cognitive function, assessed in the novel object recognition test, through kinase inhibition in three DS mouse models overexpressing DYRK1A

To investigate the importance of DYRK1A in cognitive deficits shown by transgenic mouse models of DS, we used a series of low molecular weight pharmacological inhibitors, collectively known as leucettines (Debdab et al., 2011; Tahtouh et al., 2012; Tahtouh et al., in preparation). We selected the well-characterized leucettine L41 as an archetype of this inhibitors family (Fig. 1) and L43, a closely related analogue which displays little kinase inhibitory action. Since both compounds were found to inhibit CNR1 (Tahtouh et al., in preparation), we also used L99, a DYRK1A inhibitor lacking activity on CNR1 (Fig. 1). To ensure its brain bioavailability, L41 was dosed following acute ip injection in Tg(*Dyrk1a*) and wt (wild-type) mice. Plasma half-life was about 45 min and the inhibitor reached a maximum brain concentration at 20 min., and was eliminated 2 h later. No differences in L41 pharmacokinetics or biodistribution were observed between transgenic and wt mice (Suppl. Data, Fig. S1).

We used the three mouse models of DS: Tg(*Dyrk1a*) which expresses a single additional copy of DYRK1A (Guedj, Pereira et al., 2012), and Ts65Dn (Reeves, Irving et al., 1995) and Dp1Yey (Li, Yu et al., 2007) which carry Mmu16 segments encompassing *Dyrk1a* with, respectively, 89 and 101 genes homologous to Hsa21 (Gupta, Dhanasekaran et al., 2016).

Using the NOR test, we first evaluated the effects on Tg(*Dyrk1a*) animals following daily ip treatment with L41 (20 mg/kg) for 5, 12 or 19 days (Fig. 2A). As expected, untreated wt mice discriminated the novel over the familiar object. L41 treatment for 5, 12 or 19 days had no effect on the performance of wt animals. Untreated Tg(*Dyrk1a*) mice were unable to discriminate the novel over the familiar object (Torre et al. 2014) (Fig. 2A). (Torre et al.

2014). In contrast, L41 treated Tg(*Dyrk1a*) preferentially explored the novel object, thus reversing to the behaviour of wt animals. This recovery was fully observed following 19 days treatment, but consistently or only marginally seen following 12 and 5 days treatment, respectively (Fig. 2A). In other words, a minimum of 12 days of daily L41 treatment was necessary for full recovery in the NOR test.

These experiments were repeated (daily ip treatment for 19 days) with the kinase inactive/CNR1 active L43 and the kinase active/CNR1 inactive L99 leucettines (Fig. 2B). Results clearly show the beneficial behavioural effects of L99 (Fig. 2B, right) and the lack of effects of L43 (Fig. 2B, left), demonstrating that the rescuing activity of leucettines derives from kinase inhibition rather than CNR1 antagonism.

We next ran the same experiments in Ts65Dn and Dp1Yey animals (Fig. 2C). A daily ip treatment with L41 for 19 days led to rescue in the NOR test.

Intriguingly, L41 treatment had no restoring effect on working memory (Suppl. Data, Fig. S2A) nor on place memory in Tg(*Dyrk1a*) mice (Suppl. Data, Fig. S2B), as assessed in the Y-maze and the Place Object Location paradigms, respectively.

L41 treatment has a global effect on brain functional connectivity measured by rsfMRI

To non-invasively investigate whether DYRK1A kinase activity alters the brain functional connectivity (FC) and to reveal possible circuitry based mechanisms underlying cognitive improvements induced by L41, we performed brain rsfMRI experiments in vehicle or L41 treated Dp1Yey and wt mice. The brain connectivity patterns associated with default mode network (DMN) - the main functional circuitry describing the brain's intrinsic activity at rest (Raichle, 2015) - were mapped comparatively for each experimental group (Fig. 3A-a,b and Fig. 3B-a,b) via seed based analysis. The seed used for generating DMN was retrosplenial cortex (RSP) considered as the mouse DMN core area. DMN configuration obtained for the wt vehicle-treated group (Fig. 3A-a) served as control pattern and encompassed the midline cortical areas (RSP, posterior parietal association areas (PTLp), temporal association areas (TEa), visual areas (VIS)) as well as rostral and medial anterior cingulate cortex (ACA) and hippocampal formation (HF) as previously described in mice (Sforazzini, Schwarz et al., 2014, Stafford, Jarrett et al., 2014). This DMN-like configuration was only minimally impacted by L41 treatment in wt animals (Fig. 3A-c,d), by decreasing the RSP connectivity with limited hippocampal (HF) areas.

In Dp1Yey mice, trisomy strongly influenced DMN architecture (Fig. 3Ba) by altering its pattern along midline cortical areas and highlighting pathological features of Dp1Yey brain, as compared to wt brains (Fig. 3A-a). Notably, Dp1Yey mice show reversed connectivity features of RSP (the core area of DMN) towards the rostro-frontal cortical regions, including ACA (Fig. 3A-a *vs.* Fig. 3B-a; switch from positive correlations (red/yellow scale) to negative correlations (blue scale)). Intergroup statistics (vehicle-treated wt vs. vehicle-treated Dp1Yey, Fig. S3) revealed diminished RSP-ACA connectivity in Dp1Yey animals compared to controls (Fig. S3A) while strengthening the local connectivity around RSP seed (Fig. S3B). Concurrently, the RSP of Dp1Yey-vehicle animals showed increased connectivity to limbic areas of basal forebrain (i.e. Pallidum (PAL) when referred to wt-vehicle group (Fig. S3B).

L41 treatment of Dp1Yey mice rescued this altered DMN pattern (Fig. 3B-b), prominently acting to significantly increase the FC of RSP with ACA, prefrontal cortex (PFC) and ventral HF (group statistics in Fig. 3B-d, orange/red) and to reduce FC with subcortical regions including thalamus (TH) and pallidum (PAL) (Fig. 3B-d, green/blue).

To further reveal FC signatures of L41 action in Dp1Yey mice we evaluated the connectivity, across the whole brain, for several key brain areas involved in learning and memory (hippocampal CA1 and DG areas, Perirhinal cortex, PERI and ACA).

Group statistical analysis of FC maps highlighted overall restricted effects of L41 on brain FC of wt animals (Fig. 3C-a,b,c,d) but robust L41-dependent brain FC modifications in DS model (Fig. 3D-a,b,c,d). Acting at hippocampal level, L41 treatment triggered robust changes of CA1 and DG connectivity in DS model (Fig. 3D-a,b). CA1 strengthened its FC with PFC and ACA (Fig. 3D-a, orange/red) and decreased its functional communication with ventral HF (subiculum) and thalamic nuclei (Fig. 3D-a, green/blue). The strongest L41-triggered DG connectivity modifications were identified along DG-RSP functional pathway in DS model (Fig. 3D-b). A divergent and limited effect of decreased CA1-ACA connectivity was measured in wt mice, after L41 treatment (Fig. 3C-a, green/blue), while DG altered its connectivity towards TH and superior colliculus (SC) in wt animals.

Furthermore, L41 treatment triggered remodelling of functional cross-talk between PERI cortex and HF, RSP and PTLp in Dp1Yey (Fig. 3D-c), while acting primarily on PERI cortex-TH connectivity in wt animals (Fig. 3C-c).

Group statistics additionally revealed a selective impact of L41 on ACA connectivity in Dp1Yey (Fig. 3D-d), significantly modifying its patterns towards PFC (decrease), RSP (increase), SC (increase) and hypothalamic (HY) areas (decrease). Meanwhile, L41 induced limited effects in wt mice, by decreasing ACA-PFC connectivity (Fig. 3C-d). Overall, these results indicate the potential of L41 to act at circuitry level, modifying the global brain FC in Dp1Yey mice, strongly susceptible to its effects.

Increased DYRK1A expression and catalytic activity in DS models. Leucettines normalize DYRK1A activity.

To validate the Tg(*Dyrk1a*) and Ts65Dn in terms of DYRK1A expression and function, we first verified the expression levels of *Dyrk1a* mRNA (Fig. 4A) and DYRK1A protein (Fig. 4B) in brains derived from control or L41-treated animals (19 days, daily ip). Total mRNAs were extracted from brains and *Dyrk1a*, *Gsk-3β* and *Rplp0* mRNAs were quantified by Q-PCR with specific primers. Results showed the expected ~1.5 fold increase of *Dyrk1a* mRNA levels (normalized with respect to *Gsk-3β* and *Rplp0*) in both transgenic models compared to their wt littermates. L41 treatment for 19 days did not modify *Dyrk1a* mRNA levels (Fig. 4A). DYRK1A protein levels were also increased in transgenic mice models compared to control wt animals, as shown by Western blotting (WB) of total brain proteins, while GSK-3α/β and β-actin levels remained at identical levels in transgenic and wt mice brains (Fig. 4B). L41 treatment had no effect on the expression of DYRK1A and GSK-3α/β. We next measured DYRK1A catalytic activities from transgenic and wt brain protein extract (Fig. 4C). After 19 days of L41 or vehicle treatment, GSK-3α/β activity remained identical in the brains of transgenic and wt mice (not shown), and was thus used to normalize the DYRK1A kinase activity. As expected, DYRK1A activity was elevated by ~1.5-1.8 fold in transgenic brains compared to DYRK1A activity in wt brains (Fig. 4C). L41 treatment did not reduce DYRK1A activity in wt mice brains, while it reduced DYRK1A activity by ~30% in the brains of Tg(*Dyrk1a*) and Ts65Dn animals, essentially down to the level of control counterparts. DYRK1A kinase activity was thus normalized by L41 treatment (Fig. 4C). In other words, while basal DYRK1A activity in trisomic and disomic mice brains was insensitive to L41, only excess DYRK1A activity in trisomic mice brains appeared to be sensitive to L41. To verify that all brain DYRK1A activity can in principle be inhibited by L41, DYRK1A was extracted and immunopurified from brains of untreated wt and both transgenic animals. DYRK1A kinase activities were assayed *in vitro* in the presence of increasing concentrations of L41. Results showed that wt and transgenic animal brains'

DYRK1A can be almost fully inhibited *in vitro* with essentially identical dose-response curves (Fig. 4D).

DYRK1A activity was measured following immunoprecipitation (and normalization on the basis of GSK-3 activity measured in the same samples) from brain extracts of wt and Tg(*Dyrk1a*) animals treated daily for 5, 12 or 19 days (Fig. 5A-C) with L41 or for 19 days with kinase-inactive L43 (Fig. 5D). As expected, DYRK1A activity was increased in Tg(*Dyrk1a*) vs. wt brains. Tg(*Dyrk1a*) brain DYRK1A was normalized after treatment with L41 for 12 and 19 days, but not 5 days nor after 19 days of L43 treatment. These results correlate L41 induced DYRK1A activity normalization (Fig. 5) and cognitive rescue (Fig. 2).

In all previous experiments, brains were collected 1 h following the last leucettine treatment. We wondered about the persistence of L41's effects after the last injection (Fig. 6). Tg(*Dyrk1a*) and wt animals were treated with L41/vehicle daily for 19 days. NOR tests were run and brains collected 24 or 48 h after the last L41 treatment. DYRK1A catalytic activity was dosed in Tg(*Dyrk1a*) and wt mice brains. As expected, wt brain DYRK1A activity was insensitive to L41 treatment. Tg(*Dyrk1a*) brain DYRK1A activity was increased compared to control wt (Fig. 6A, 6C) and normalized to wt levels 24 h after the last L41 treatment (Fig. 6A). In contrast L41 had no more effects 48 h after the last treatment (Fig. 6C). In terms of restoration of cognitive abilities, the NOR tests revealed that Tg(*Dyrk1a*) deficits were still corrected 24 h, but not 48 h, after the last L41 treatment (Fig. 6B, 6D). Since L41 is essentially undetectable in brain extracts 2 h after the acute ip injection, it may either be protected from degradation once bound to DYRK1A or it may have been metabolized to an unidentified, stable active inhibitor.

Overexpressed DYRK1A accumulates in cytoplasm and synapse. Differential subcellular L41 distribution.

We next investigated the subcellular distribution of DYRK1A in the brains of Tg(*Dyrk1a*) and wt animals (Fig. 7A, 7B). Brains were collected and cells dissociated and fractionated using two methods. The first allowed the separation of a cytosol + synaptosomes fraction from a nuclear fraction (Fig. 7A). The second separated a cytosol + nuclei fraction from a synaptosomal fraction (Fig. 7B). The purity of each fraction was evaluated by WB with specific markers: postsynaptic density protein 95 (PSD95) (cytosol + synaptosomes), histone H2B (nuclei), cyclin L1 (cytosol + nuclei), synapsin1 (SYN1) and AMPA-selective glutamate receptor 1 (GLUR1) (synaptosomal fraction) (Fig. 7A & 7B, top panels). DYRK1A expression levels were assessed following SDS-PAGE of the different cellular fractions

followed by WB, and normalization with the levels of B-actin (Fig. 7A & 7B, lower panels). DYRK1A was detected in all fractions in both genotypes, but its expression was significantly higher, by a ~1.5 fold factor, in the cytosol and synaptosomes of Tg(*Dyrk1a*) brains compared to wt brains. No difference in nuclear DYRK1A expression was seen between transgenic and wt animals. Brain DYRK1A overdosage in Tg(*Dyrk1a*) animals thus occurs in the cytosol and synaptosomes, but not in the nuclei. We are currently exploring the reasons for this differential distribution of excess DYRK1A.

We next measured L41 levels in nuclear and cytoplasmic fractions prepared from brains of Tg(*Dyrk1a*) and wt animals which had been ip injected daily for 19 days with L41 (20 mg/kg) or vehicle (Fig. 7C, 7D). At the end of the treatments, brains were recovered and processed for L41 extraction and quantification by isobaric stable isotope chemical labelling (iTRAQ) followed by ultra-precision liquid chromatography/mass spectrometry. Results show essentially undetectable L41 in vehicle-treated animals, identical L41 levels in the brain nuclear fractions of Tg(*Dyrk1a*) and wt animals (Fig. 7C) and a significantly increased L41 level in the cytoplasmic fraction of Tg(*Dyrk1a*) brains compared to the cytoplasmic fraction of wt animals brains (Fig. 7D). Thus DYRK1A overexpression in the transgenic animals' brains appears to be limited to the cytoplasmic fraction, corresponding to the subcellular distribution of overexpressed DYRK1A (Fig. 7A, 7B). Accordingly more L41 is detected in the cytoplasmic fraction from transgenic animal compared to control littermate.

Phosphoproteomic impacts of DYRK1A trisomy and L41 treatment reveal key synaptic and cytoskeletal components

To explore the mechanisms of action of L41 underlying its correcting effects on NOR cognitive deficits of transgenic models, we analysed the phosphoproteome of proteins isolated from hippocampus, cortex and cerebellum of both Tg(*Dyrk1a*) and Ts65Dn models, with their respective wt counterparts and following treatment with vehicle or L41 (20 mg/kg, daily ip injection for 19 days) (Fig. 8). All tissue samples were processed for phosphoproteomics analysis (see Material & Methods section). Tg(*Dyrk1a*) and Ts65Dn mice hippocampus, cortex and cerebellum respectively yielded 1384, 1523 and 2004 peptides, corresponding to 886, 948 and 1229 proteins (Table 1; Supplementary Tables S1-S12).

Among the peptides/proteins detected in this study, only 30% of the proteins and 20% of the peptides were significantly up- or down- regulated in trisomic vs. wt animals. Most peptides (80%) were phosphorylated on serine residues, while phosphorylation on threonine (15%) or tyrosine residues (5%) were less frequent. Less than 5% were phosphorylated on

two amino acids. Very few phosphopeptides displayed the consensus DYRK1A phosphorylation sequence (R-P-x(1,3)-S/T-P) and most phosphopeptides were predicted to be phosphorylated by kinases from the CMGC (MAPK or GSK-3) or AGC (MTOR or PKG) groups (data obtained with the PhosphoRS algorithm within the Proteome Discoverer software tool, version 1.4).

We selected the phosphopeptides displaying a trisomy-associated modulation (up- or down-regulation) which was reverted by L41 treatment (down- or up-regulation) (Fig. 8). These analyses were first run in each brain tissue and in each of the two models and their wt controls. We thus focused on proteins displaying an L41 reversible, trisomy-associated phosphorylation modulation. Based on these two criteria, 258 and 248 phosphoproteins were selected from Tg*(Dyrk1a)* and Ts65Dn hippocampus (Fig. 8A), respectively. Similarly, the Tg*(Dyrk1a)* and Ts65Dn cortex respectively showed 238 and 223 dysregulated phosphoproteins (Fig. 8A). 330 and 341 phosphoproteins in Tg*(Dyrk1a)* and Ts65Dn cerebellum, respectively, were found to be altered by trisomy and L41 treatment (Fig. 8A). Among these phosphoproteins, 102, 88 and 124 were common to both transgenic models in the hippocampus, cortex and cerebellum, respectively (Supplementary Tables S1-S12). These shared phosphoproteins were selected for DAVID cluster analysis (Supplementary Tables S10-S12) which unravelled enrichment in synaptic, cytoskeletal and learning pathways (Fig. 8B, Supplementary Fig. S4). Toppcluster analysis of the modulated phosphoproteins in each model and each brain region confirmed enrichment in synaptic transmission common to both models in hippocampus and cortex, while cytoskeleton organization was enriched in both models for all three brain regions (Fig. 8B) (Supplementary Tables S11-S13).

We also compared, in each model, the phosphoproteins subsets of all three brain areas (Fig. 8C). In Tg*(Dyrk1a)*, only 16 phosphoproteins were commonly modulated in the three brain sub-structures (Fig. 8C, left), while only 22 responded to these criteria in Ts65Dn (Fig. 8C, center). Among these 16 and 22 phosphoproteins shared by the three brain regions, only 5 were common to both DS models (Fig. 8D): the microtubule associated proteins MAP1A, MAP1B, MAP2 and presynaptic components Piccolo (PCLO) and SYN1. All phosphosites modulated by both trisomy and L41 treatment, for each of the 5 proteins, are schematized in Suppl. Fig. 3. They illustrate the complexity of the phosphoproteomics consequences of a single gene trisomy (Tg(*Dyrk1a*)) or a partial chromosome 16 trisomy (Ts65Dn) and the complexity resulting from the treatment with a single pharmacological agent. Among these 5 proteins, we looked for the residues up-phosphorylated when DYRK1A was over-expressed and down-regulated when DYRK1A was inhibited by L41, and also matching the consensus

DYRK1A phosphorylation sequence (Himpel et al. 2000). Based on these criteria, Serine 551 of SYN1 was selected for further study.

DYRK1A interacts with SYN1 and other proteins implicated in synaptic functions

To investigate potential interactions between DYRK1A and SYN1, co-immunoprecipitation (co-IP) experiments were carried out with adult mouse brain lysates (Fig. 9A) using antibodies directed against SYN1 or DYRK1A (negative control: GAPDH). As expected, DYRK1A and SYN1 were found in their respective immunoprecipitates (IPs). SYN1 was detected in DYRK1A IPs and DYRK1A was detected in SYN1 IPs (Fig. 9A), suggesting that these proteins form a direct or indirect complex in brain extracts. Calmodulin-dependent kinase 2A (CAMK2A) was present in SYN1 IPs, as expected from previous results (Llinás et al. 1985; Fabio Benfenati et al. 1992) and from its role in presynaptic vesicle pool release (Cesca et al. 2010). CAMK2A was also detected in DYRK1A IPs, suggesting the possibility of a DYRK1A/SYN1/CAMK2A complex, although separate DYRK1A/CAMK2A and SYN1/CAMK2A complexes are possible.

To see whether DYRK1A directly phosphorylates SYN1, we ran *in vitro* kinase assays using recombinant DYRK1A and various SYN1 derived peptides, comprising Ser551, as potential substrates or Woodtide as a reference substrate (Fig. 9B, 9C). Recombinant DYRK1A displayed similar activity towards SYN1-tide or SYN1-S553A-tide compared to Woodtide. In contrast, no significant phosphorylation could be measured with the SYN1-S551A peptide. This confirms that DYRK1A is able to phosphorylate SYN1 on its S551 residue, but not on the nearby Ser553 site. This site corresponds to the consensus DYRK1A phosphorylation site (Fig. 9B).

DISCUSSION

Rescue of cognitive deficits by pharmacological inhibition of excess DYRK1A

In this study we show that trisomy is associated with an increase in DYRK1A expression and catalytic activity, and that a class of synthetic DYRK1A inhibitors, Leucettines, exemplified with L41, is able to cross the blood brain barrier (BBB) and selectively inhibit the excess DYRK1A linked to trisomy. Why only this fraction of overexpressed DYRK1A is inhibited, and most native, basal DYRK1A is not, remains a mystery. This effect may be linked to the accumulation of excess DYRK1A and L41 in specific cellular compartments and not in others, as shown in Fig. 7. Intriguingly, a similar sensitivity to inhibition of excess DYRK1A compared to ‘normal’ DYRK1A was observed with EGCG. This finding is encouraging in terms of potential therapeutic implications, as

complete inhibition of DYRK1A is not desired. Intracellular DYRK1A has been described in both nuclear and cytoplasm compartments (Martí et al. 2003), we are adding synaptosomes, a fact that may have essential consequences (see below).

We here demonstrate the rescuing effect of synthetic DYRK1A inhibitors, Leucettines L41 and L99, on deficient recognition memory of three different trisomic mouse models with increasing genetic complexity, Tg(*Dyrk1a*), Ts65Dn and Dp1Yey. These beneficial behavioural effects directly correlate with inhibition of excess DYRK1A activity. There is also a strong coincidence with duration of the drug treatment (Fig. 2A, 5), potency of leucettine analogues (Fig. 2B, 5) and duration of the drug-free period following the last injection (Fig. 6). Finally, behavioural correcting benefits detected in the NOR test (Fig. 2, 6) correlate with remodelling of brain functional connectivity detected by fMRI (Fig. 3). However, we observed that working and spatial memories impaired in the Tg(*Dyrk1a*) mice were insensitive to L41 treatment as respectively assessed in the Y-maze and the Place Object Location task. This indicates a specific action of DYRK1A inhibition on molecular pathways specifically related to recognition memory. Our findings further strengthen the essential role played by DYRK1A in intellectual phenotypes associated with DS. Leucettine derivatives should be investigated further as drug candidates to improve cognitive functions of DS patients.

L41 treatment in DYRK1A overexpressing mice triggers remodelling of brain FC pathways

Brain rsfMRI in Dp1Yey mice revealed global resilience of functional cerebral circuitry after L41 administration. Notably, L41 corrected the abnormal DMN patterns found in Dp1Yey mice, but also acted on connectivity of key brain areas associated to cognitive and memory processing (PFC, ACA, PERI, HF). DMN (Raichle 2015b) – previously described as a highly active circuitry during rest - and preserved across species (Stafford et al., 2014), was shown to be vulnerable to various neuropathological conditions (Hawellek, Hipp et al., 2011, Raichle, 2015, Zhou, Friston et al., 2017), including DS (Anderson, Nielsen et al., 2013, Pujol, del Hoyo et al., 2015). The core area of this network in mice is RSP (associated to posterior cingulate/precuneus cortex in humans) (Hübner, Mechling et al., 2017, Sforazzini et al., 2014). Our analysis unravelled increased local connectivity around RSP in DS mice, but strongly reduced long-range communication with fronto-cortical brain regions (ACA, PFC - Fig. S3), when compared to wt animals. This short-range stronger connectivity is not limited to RSP, but represented a common feature for other investigated brain regions (ACA, PERI,

HF) of Dp1Yey mice. Such pattern of increased local, short range brain communication was described as cardinal feature of FC in DS patients (Anderson et al., 2013, Pujol et al., 2015, Vega, Hohman et al., 2015). Indeed, DS human brains are characterized by simplified network structure, organized by local connectivity (Anderson et al., 2013, Pujol et al., 2015, Vega et al., 2015) and impaired efficiency to integrate information from distant connections.

Dp1Yey mouse brains additionally displayed features of higher negative functional correlations as compared with wt vehicle group and more obviously a reversed correlation pattern (switch from positive to negative correlations) between RSP and frontal cortical areas in the DS model. This feature, attenuated or corrected following L41 treatment, could eventually be discussed in the context of L41 regulation of inhibition/excitation ratios, imbalanced in DYRK1A overexpressing mice (Souchet, Guedj et al., 2014). Indeed, increased number and increased signal intensity from neurons expressing GAD67, an enzyme that synthesizes GABA, indicating inhibition pathway alterations, was quantified in three different DS models (Souchet et al., 2014), including Dp1Yey. Pharmacological correction of inhibition/excitation was achieved in Tg(*Dyrk1a*) DS mouse model (Souchet, Latour et al., 2015) by EGCG treatment. We can speculate on a similar effect of L41 on inhibition/excitation balance, and subsequent modulation of brain connectivity. Nevertheless, the brain synchrony modifications after L41 inhibition of excess DYRK1A activity in DA model may potentially reflect other molecular mechanisms and interactions at synaptic and cytoskeletal level as shown here, and subsequently underpin correction of cognitive and memory deficits of DS mice. Importantly, L41 had only limited effects on FC of wt animals, whereas in Dp1Yey model it largely impacted the connectivity features, on distributed action sites, that coincide with alterations reported for brain anatomy in DS models, most notably, frontal and prefrontal cortical areas (ACA/PFA), HF, PAL and TH. Volumetric MRI in DS mouse models, showed a general trend of smaller frontal lobes, hippocampal and cerebellar regions, but larger thalamic and hypothalamic areas (Powell, Modat et al., 2016, Roubertoux, Baril et al., 2017). Diffusion MRI also identified potential mictrostructural alterations in above mentioned areas and also striatum (including PAL) (Nie, Hamlett et al., 2015). Our rsfMRI study advances the current knowledge on the brain functional communication in DS mouse models, revealing targeted and effective action of L41 on brain circuitry, consistent with the profile of cognitive and novel object recognition memory improvements.

DYRK1A and Synapsin 1

Phosphoproteomic analyses using ultra-high precision LC-MS analysis unravelled several clusters of neuronal phosphorylated proteins directly controlled by DYRK1A or clusters indirectly modulated in the trisomic condition and sensitive to L41 treatment. 5 phosphoproteins were shared by Tg(*Dyrk1a*) and Ts65Dn mice and were present in three brain substructures (hippocampus, cortex, cerebellum) (Fig. 8). Furthermore these phosphoproteins showed significant modulation in their phosphorylation level in trisomic vs. disomic animals and these modulations were sensitive, in the opposite direction, to L41 treatment. A few key pathways, including controlling synaptic vesicle transport, calcineurin NFAT signalling and cytoskeleton organisation, were found to be directly affected by DYRK1A, or as a consequence of its kinase activity (Suppl. Fig. S4), while other may represent indirect effects of the overdosage. Nevertheless the immune response was found to be affected, correlating with several studies linking DYRK1A to inflammation. We here focussed on SYN1 as it was the only protein that revealed a serine residue corresponding to the DYRK1A phosphorylation consensus sequence. SYN1 Ser551 was hyperphosphorylated following DYRK1A overexpression and dephosphorylated following L41 treatment. Representative annotated ultra-high resolution product ion spectrum of proteotypic peptide qSRPVAGGPGAPPAARPPAsPSPqR encoding the phosphorylated residue Ser551 is shown in Fig. S6.

Co-IP experiments showed that DYRK1A interacts, either directly or indirectly, with SYN1 (Fig. 9). SYN1 has been described to be involved in the reserve synaptic vesicle (SV) pool maintenance at the presynaptic bouton by tethering SVs to the actin cytoskeleton (Hilfiker et al., 2005; F. Benfenati, Valtorta, and Greengard 1991). Phosphorylation of SYN1 by CAMKII leads to the release of SVs and allows them to move close to the active zone (Llinás et al. 1991). Neurotransmitter release at the active zone is thus strongly dependent on SYN1 phosphorylation. We showed that SYN1 was phosphorylated by DYRK1A on its S551 residue *in vitro* and *in vivo*, thus highlighting a novel role of DYRK1A in SYN1-dependent presynaptic vesicle trafficking. Beside its physiological role in synaptic plasticity regulation, SYN1 has been associated with epilepsy (Garcia et al. 2004; Fassio et al. 2011). Mutations in phosphorylation domains of SYN1 essential for vesicle recycling control have been related to epilepsy (Fassio et al., 2011). In addition, MRD7 (mental retardation, autosomal dominant 7) patients with *Dyrk1a* happoinsufficiency display epilepsy seizures (Courcet et al. 2012; Møller et al. 2008; Oegema et al. 2010; Valetto et al. 2012; Yamamoto et al. 2011). Our

results suggest that epileptic seizures observed in MRD7 patients may be induced by defects in SYN1 regulation.

DYRK1A, microtubule-binding proteins, Piccolo and other synaptic targets

The other 4 proteins found in our phosphoproteomics study will be the object of another study but are briefly reviewed here. The detection of MAP1A, MAP1B, MAP2, all previously reported as DYRK1A substrates (Murakami et al. 2012; Scales et al. 2009), validated the power of our analysis and confirmed the role of DYRK1A in dendrite morphogenesis and microtubule regulation (Ori-McKenney et al. 2016). The last phosphoprotein, Piccolo, is a cytoskeletal matrix protein associated with the presynaptic active zone (Cases-Langhoff et al. 1996) which acts as a scaffolding protein implicated in SV endocytosis and exocytosis (Garner, Kindler, and Gundelfinger 2000; Fenster et al. 2003). The lack of PCLO in the human brain leads to a dramatic neuronal loss associated with pontocerebellar hypoplasia type III (Ahmed et al. 2015). Moreover, PCLO knockdown in cultured hippocampal neurons increases SYN1A dispersion out of the presynaptic terminal and synaptic vesicles exocytosis (Leal-Ortiz et al. 2008). It has been shown that PCLO modulates neurotransmitter release by regulating F-actin assembly (Waites et al. 2011). It clearly appears that PCLO acts upstream of SYN1 and regulates its role in vesicle recycling.

Taken together, our findings reveal Synapsin 1 as a new direct substrate of DYRK1A, suggesting a novel role of this kinase in the regulation of SV release at the presynaptic terminal. Moreover, the relatively safe and selective DYRK1A inhibitors Leucettines successfully correct recognition memory deficits associated with DS in three different mice models. Although the DYRK1A-dependent biological process which is rescued by these drugs still needs to be elucidated, Leucettines and their analogues represent promising therapeutic drugs to enhance cognitive functions in DS patients.

There is strong support for the involvement of DYRK1A in cognitive deficits associated with Alzheimer's disease (AD): (1) DYRK1A mRNA (Kimura et al., 2007) and protein (Ferrer et al, 2005) levels are increased in post-mortem human AD brains compared to healthy brains, (2) calpain I -induced cleavage of DYRK1A is observed in AD brains and associated with increased activity (Jin et al., 2015), (3) DYRK1A phosphorylates key AD players, such as amyloid precursor protein (Ryoo et al., 2008), presenilin 1 (Ryu et al., 2010), Tau (Woods et al., 2001; Ryoo et al., 2007; Azorsa et al., 2010; Coutadeur et al., 2015; Jin et al., 2015), septin (Sitz et al., 2008) and neprylysin (Kawakubo et al., 2017), (4) DYRK1A regulates splicing of Tau mRNA (Shi et al., 2008; Wegiel et al., 2011; Yin et al., 2012, 2017;

Jin et al., 2015), (5) DYRK1A inhibition corrects cognitive defects in 3xTG-AD (Branca et al., 2017), APP/PS1 (Souchet et al., in preparation) and Aβ25-35 peptide injected wt mice (Naert et al., 2015), three widely used mice models of AD. These facts provide additional incentive to investigate the regulation and substrates of brain DYRK1A and to develop potent and selective DYRK1A inhibitors to treat cognitive deficits observed in different indications. DS patients display early symptoms of AD and show a high frequency of dementia at later age (Ballard et al. 2016). The triplication of APP located on the HSA21 is thought to generate amyloid plaques and neurofibrillary tangles, two causative factors in AD, that possibly accumulate early in 30-40 years old DS people (Head, Powell, et al. 2012). These factors, associated with neuroinflammation and oxidative damage also diagnosed in both AD and DS individuals, lead to precocious dementia observed from age 30-39 (Head, Silverman, et al. 2012). Studying DS will have impact on the understanding of AD and reciprocally, and DYRK1A is clearly a common factor between the two diseases.

MATERIALS AND METHODS

Animal model, treatment and behaviour assessment

Tg(*Dyrk1a*) mutant mice and Dp1Yey models were maintained on the C57BL/6J genetic background. Ts(17^{16})65Dn trisomic mice were obtained from the Jackson laboratory and kept on the C57BL/6J x C3B, a congenic sighted line for the BALB/c allele at the *Pde6b* locus (Hoelter, Dalke et al., 2008). The local ethics committee, Com'Eth (n°17), approved all mouse experimental procedures, under the accreditation number APAFIS #5331 and #3473 with YH as the principal investigator in this study.

Behavioural studies were conducted in 12-20 week old male animals. All assessments were scored blind to genotype and treatment as recommended by the ARRIVE guidelines (Karp, Meehan et al., 2015, Kilkenny, Browne et al., 2010). Leucettine L41 was prepared at 40 mg/mL in DMSO (dimethylsulfoxide), aliquoted and stored below -20°C. The final formulation was prepared just prior to use as a 2 mg/mL solution diluted in PEG300/water (50/45), to reach a final DMSO/PEG300/water 5/50/45 (v/v/v) mix. Treated animals received a daily dose (5, 12 or 19 days) of this formulation by intra-peritoneal injection of 20 mg/kg/day. Non-treated animals received the same formulation without L41.

The NOR task is based on the innate tendency of rodents to differentially explore a novel object over a familiar one (Ennaceur & Delacour, 1988). Day 1 was an habituation session. Mice freely explored the apparatus, a white circular arena (53 cm diameter) placed in a dimly lit testing room (40 lux). On day 2, the acquisition phase, mice were free to explore two identical objects for 10 min. Mice were then returned to their home cage for a 24 h retention interval. To test their memory, on day 3, one familiar object (already explored during the acquisition phase) and one novel object were placed in the apparatus and mice were free to explore the two objects for a 10 min period. Between trials and subjects, the different objects were cleaned with 50° ethanol to reduce olfactory cues. To avoid a preference for one of the objects, the new object was different for different animal groups and counterbalanced between genotype and treatment as well as for location of novel and familiar objects (left or right). Object exploration was manually scored and defined as the orientation of the nose to the object at a distance <1 cm. For the retention phase, the percent of time spent exploring familiar vs. novel objects was calculated to assess memory performance.

Resting state magnetic resonance imaging (rsfMRI)

rsfMRI was performed on 26 animals separated in 4 groups: wt, vehicle treated; wt, L41 treated; Dp1Yey, vehicle treated; Dp1Yey, L41 treated. RsfMRI was carried under medetomidine sedation during scanning (subcutaneous bolus injection, 0.3 mg/kg in 100 µL 0.9% NaCl solution right before the scan followed by continuous subcutaneous infusion of medetomidine (0.6 mg/kg, 200 µL/h). Physiological parameters were continuously monitored. RsfMRI data was collected using a 7 T small bore animal scanner and a mouse head adapted cryocoil (Biospec 70/20 and MRI CryoProbe, Bruker, Germany). The whole brain was examined (24 slices: 150 × 150 x 700 μm^3 spatial resolution) using single shot gradient echo EPI (TE/TR = 10 ms/1700 ms). 200 volumes were recorded. The preprocessing included: motion correction, data co-registration with Allen mouse brain atlas (AMBA), detrending, band pass filtering (0.01 - 0.1 Hz) and regression of ventricular signal. For seed-based correlation analysis, the functional connectivity of several brain areas was mapped: restrosplenial (RSP) cortex to map the default mode network, CA1, dentate gyrus, perirhinal cortex and anterior cingulate area (ACC). Correlation coefficients were then computed (two-tailed t-test, $p < 0.001$) between the seed region and the averaged BOLD signal time series of the remaining whole brain for each group and were converted and mapped to z values using Fisher's r-to-z transformation.

DYRK1A and GSK-3β protein levels

Brains were obtained from mice and snap-frozen until further use. Then tissues were weighed, homogenized and sonicated in 1 mL lysis buffer (60 mM β-glycerophosphate, 15 mM p-nitrophenylphosphate, 25 mM Mops pH 7.2, 15 mM EGTA, 15 mM $MgCl_2$, 2 mM dithiothreitol, 1 mM sodium orthovanadate, 1 mM sodium fluoride, 1 mM phenylphosphate disodium and protease inhibitor cocktail) per g of material. Homogenates were centrifuged for 15 min at 17,000 g and 4°C. The supernatant was recovered and assayed for protein content (Biorad, France). The proteins were separated by 10% NuPAGE pre-cast Bis-Tris polyacrylamide mini gel electrophoresis (Invitrogen, France) with MOPS-SDS running buffer. Proteins were transferred to 0.45-µm nitrocellulose filters (Schleicher & Schuell, Whatman, Dessel, Germany). They were blocked with 5% low-fat milk in Tris-buffered vehicle/Tween-20, incubated overnight at 4°C with antibodies. Anti-DYRK1A (H00001859-M01, 1:1000) and anti-GSK-3 α/β (KAM-ST002E, 1:1000) were obtained from Interchim (France) and Stressgen (France), respectively. Appropriate secondary antibodies conjugated to horseradish peroxidase (BioRad, France) were added to visualize the proteins using the Enhanced Chemiluminescence reaction (ECL, Amersham, France).

Protein kinase assays

Protein kinase assays to measure the catalytic activity of DYRK1A in brains of the animals treated or not with drugs were performed as follows: frozen half brains were homogenized in lysis buffer (1.2 mL/half brain) using Precellys® homogenizer tubes. After centrifugation at 5,000 rpm for 2 x 15 s, 1 mg of brain extract was incubated with 2 µg DYRK1A (H00001859 M01, Interchim, France) or GSK3-β (MBS8508391, Emelca Bioscience, France) antibodies at 4°C for 1 h under gentle rotation. 20 µL of Protein G Agarose beads (Thermo Fisher Scientific, France), previously washed three times with bead buffer (50 mM Tris pH 7.4, 5 mM NaF, 250 mM NaCl, 5 mM EDTA, 5 mM EGTA, 0.1% Nonidet P-40 and protease inhibitor cocktail from Roche, France), were then added to the mix and gently rotated at 4°C for 30 min. After a 1 min spin at 10,000 x g and removal of the supernatant, the pelleted immune complexes were washed three times with bead buffer, and a last time with Buffer C (60 mM β-glycerophosphate, 30 mM p-nitrophenolphosphate, 25 mM Mops pH 7.2, 5 mM EGTA, 15 mM MgCl2, 2 mM dithiothreitol, 0.1 mM Na Orthovanadate, 1 mM phenylphosphate, protease inhibitor cocktail). DYRK1A or GSK-3 immobilized on beads were assayed in buffer C as described in the Supplementary Data section with

Woodtide (KKISGRLSPIMTEQ) (1.5 µg/assay) or GSK3-tide (YRRAAVPPSPSLSRHSSPHQpSED-
EEE, where pS stands for phosphorylated serine) as substrates.

Protein kinase assays to evaluate SYN1 phosphorylation by DYRK1A were performed with 50 ng of recombinant DYRK1A protein (PV3785, ThermoScientific, France) and 0.98 mM Woodtide, and three peptides derived from the synapsin 1 putative DYRK1A phosphorylation site (Fig. 9C). Kinase activity was then measured as described in the Supplementary Data.

The selectivity of the three Leucettines used in this study was evaluated in a panel of 16 recombinant protein kinases assayed as described in the Supplementary Data section.

Subcellular fractionation

Nuclear, cytosolic and synaptosomal subcellular fractionation of brain tissue was performed with the Syn-PER™ and ProteoExtract® Tissue Dissociation Buffer Kit and Subcellular Proteome Extraction Kit following the instructions of the manufacturer. Fractions were analyzed by SDS-PAGE and WB with specific antibodies.

Phosphoproteomics results analysis

Gene ontology enrichment analyses of phosphoproteins that are modulated (up- or down-regulated) in Tg(*Dyrk1a*) or Ts65Dn mice versus wt and also modulated in the opposite way (down- or up-regulated) by the L41 treatment, were conducted using ToppCluster (Bonferroni correction, P-value cutoff 0.05). Only biological processes common to the three brain regions and both models are presented (complete biological processes are listed in Supplementary Tables S11-S13).

DYRK1A substrates and their respective phosphorylation sites were identified in the phosphoproteome based on the DYRK1A phosphorylation consensus sequence R-P-x(1,3)-S/T-P (Himpel et al. 2000). Protein-protein interactions of each substrate were generated with STRING web server application. Biological process enrichments of each cluster were assessed by using ToppCluster web server application. Phospho-network was mapped with the Cytoscape tool. See Supplementary data for details.

Immunoprecipitation and immunoblotting

All immunoprecipitations were performed on fresh half brains of 3 months wt male mice. Brains were dissected and lysed in 1.2 mL RIPA lysis buffer (Santa-Cruz, France) using Precellys® homogenizer tubes. After centrifugation at 5,000 rpm for 2 x 15 s, 1 mL brain extract was incubated with 2 µg of antibody of interest at 4°C for 1 h under gentle rotation. An aliquot of the remaining supernatant was kept for further immunoblotting as homogenate control. 20 µL of Protein G Agarose beads, previously washed three times with bead buffer, were then added to the mix and gently rotated at 4°C for 30 min. After a 1 min spin at 10,000 x g and removal of the supernatant, the pelleted immune complexes were washed three times with bead buffer before WB analysis with appropriate antibodies directed against DYRK1A (H00001859 M01, Interchim, France, 1:1000), PSD95 (ab18258, Abcam, France 1:1000), SYN1 (ab64581, Abcam, France 1:1000), CAMK2A (PA5-14315, ThermoFisher Scientific, France 1:1000) and GAPDH (MA5-15738, ThermoFisher, France, 1:3000). Immunoblots were revealed with Clarity Western ECL Substrate.

ACKNOWLEDGMENTS

This research was supported by the 'Fonds Unique Interministériel" (FUI) TRIAD project and Conseil Régional de Bretagne (LM, YH, JPB), the "Fondation Jérôme Lejeune" (LM), an FP7-KBBE-2012 grant (BlueGenics) (LM), and by French state funds through the "Agence Nationale de la Recherche" ("Programme Investissements d'Avenir") [ANR-10-IDEX-0002-02, ANR-10-LABX-0030-INRT, ANR-10-INBS-07 PHENOMIN to Y.H.]. The funders had no role in study design, data collection and analysis, decision to publish nor manuscript preparation. TLN is recipient of a CIFRE/ManRos Therapeutics Ph.D. fellowship.

SUPPLEMENTARY INFORMATION

Supplementary data is available on-line. Phosphoproteomics data is provided in Supplementary Tables S1-S12.

AUTHOR CONTRIBUTIONS

TLN, SDG, LM and YH designed the study and contributed to writing of the manuscript. AD performed the initial *in vivo* experiments. TLN ran most *in vivo* experiments, most biochemical experiments and the statistical analyses. NL and TLN performed the kinase assays. AM and TLN ran phosphoproteomics experiments analyses. S.D.G. designed and supervised phosphoproteomics experiments and interpretation. BV ran mRNA quantifications, GP pharmacokinetics & genotyping and LH rsfMRI experiments & analysis. Leucettines were synthesized by EL, JPB and FC. They were characterized and provided by ManRos Therapeutics. All authors read and approved the final manuscript.

CONFLICT OF INTEREST

LM is founder, CEO and CSO of ManRos Therapeutics which licensed the patent on leucettines and develops these as DS/AD drug candidates. LM, FC and JPB are co-inventors on the leucettine patent.

THE PAPER EXPLAINED

PROBLEM. The gene encoding the DYRK1A kinase is located in the "Down syndrome (DS) critical region" of chromosome 21. Excess (1.5 fold increase) DYRK1A expression in DS patients correlates with their cognitive deficits. Increased DYRK1A activity also appears to be involved in cognitive impairment of Alzheimer's disease patients.

RESULTS. We provide a detailed proof of concept that normalization of DYRK1A catalytic activity can be achieved in three different mouse models of DS by the mere treatment with small molecule pharmacological inhibitors of DYRK1A. Consequently these inhibitors correct recognition memory deficits measured in these animal models of DS.

IMPACT. DS is still the most common form of intellectual disabilities. Even after prenatal diagnosis, the prevalence is still around 1 out of 2000 birth in industrialized countries whereas in other places the lower risk is around 1 out of 700 newborns. The development of potent, selective and well characterized pharmacological inhibitors of DYRK1A constitutes a straightforward approach to improve the cognitive abilities of DS patients. Improving cognition levels in DS patients should improve their autonomy and ability to integrate society, reducing costs and parent's anxiety.

REFERENCES

Ahmed, Mustafa Y., Barry A. Chioza, Anna Rajab, Klaus Schmitz-Abe, Aisha Al-Khayat, Saeed Al-Turki, Emma L. Baple, et al. 2015. "Loss of PCLO Function Underlies Pontocerebellar Hypoplasia Type III." *Neurology* 84 (17): 1745. https://doi.org/10.1212/WNL.0000000000001523.

Ahn, Kyoung-Jin, Hey Kyeong Jeong, Han-Saem Choi, Soo-Ryoon Ryoo, Yeon Ju Kim, Jun-Seo Goo, Se-Young Choi, Jung-Soo Han, Ilho Ha, and Woo-Joo Song. 2006. "DYRK1A BAC Transgenic Mice Show Altered Synaptic Plasticity with Learning and Memory Defects." *Neurobiology of Disease* 22 (3): 463–72. https://doi.org/10.1016/j.nbd.2005.12.006.

Altafaj, Xavier, Mara Dierssen, Carmela Baamonde, Eulàlia Martí, Joana Visa, Jordi Guimerà, Marta Oset, et al. 2001. "Neurodevelopmental Delay, Motor Abnormalities and Cognitive Deficits in Transgenic Mice Overexpressing Dyrk1A (Minibrain), a Murine Model of Down's Syndrome." *Human Molecular Genetics* 10 (18): 1915–23. https://doi.org/10.1093/hmg/10.18.1915.

Altafaj, Xavier, Eduardo D. Martín, Jon Ortiz-Abalia, Aitana Valderrama, Cristina Lao-Peregrín, Mara Dierssen, and Cristina Fillat. 2013. "Normalization of Dyrk1A Expression by AAV2/1-shDyrk1A Attenuates Hippocampal-Dependent Defects in the Ts65Dn Mouse Model of Down Syndrome." *Neurobiology of Disease* 52 (April): 117–27. https://doi.org/10.1016/j.nbd.2012.11.017.

Alvarez, Mónica, Xavier Altafaj, Sergi Aranda, and Susana de la Luna. 2007. "DYRK1A Autophosphorylation on Serine Residue 520 Modulates Its Kinase Activity via 14-3-3 Binding." *Molecular Biology of the Cell* 18 (4): 1167–78. https://doi.org/10.1091/mbc.E06-08-0668.

Anderson, Jeffrey S., Jared A. Nielsen, Michael A. Ferguson, Melissa C. Burback, Elizabeth T. Cox, Li Dai, Guido Gerig, Jamie O. Edgin, and Julie R. Korenberg. 2013. "Abnormal Brain Synchrony in Down Syndrome." *NeuroImage: Clinical* 2 (January): 703–15. https://doi.org/10.1016/j.nicl.2013.05.006.

Arron, Joseph R., Monte M. Winslow, Alberto Polleri, Ching-Pin Chang, Hai Wu, Xin Gao, Joel R. Neilson, et al. 2006. "NFAT Dysregulation by Increased Dosage of DSCR1 and DYRK1A on Chromosome 21." *Nature* 441 (7093): 595–600. https://doi.org/10.1038/nature04678.

Azorsa, David O, RiLee H Robeson, Danielle Frost, Bessie Meec hoovet, Gillian R Brautigam, Chad Dickey, Christian Beaudry, et al. 2010. "High-Content siRNA Screening of the Kinome Identifies Kinases Involved in Alzheimer's Disease-Related Tau Hyperphosphorylation." *BMC Genomics* 11 (January): 25. https://doi.org/10.1186/1471-2164-11-25.

Ballard, Clive, William Mobley, John Hardy, Gareth Williams, and Anne Corbett. 2016. "Dementia in Down's Syndrome." *The Lancet Neurology* 15 (6): 622–36. https://doi.org/10.1016/S1474-4422(16)00063-6.

Benfenati, F., F. Valtorta, and P. Greengard. 1991. "Computer Modeling of Synapsin I Binding to Synaptic Vesicles and F-Actin: Implications for Regulation of Neurotransmitter Release." *Proceedings of the National Academy of Sciences* 88 (2): 575–79.

Benfenati, Fabio, Flavia Valtorta, James L. Rubenstein, Fred S. Gorelick, Paul Greengard, and Andrew J. Czernik. 1992. "Synaptic Vesicle-Associated Ca2+/Calmodulin-Dependent Protein Kinase II Is a Binding Protein for Synapsin I." *Nature* 359 (6394): 417–20. https://doi.org/10.1038/359417a0.

Cases-Langhoff, C., B. Voss, A. M. Garner, U. Appeltauer, K. Takei, S. Kindler, R. W. Veh, P. D. C. milli, E. D. Gundelfinger, and C. C. Garner. 1996. "Piccolo, a Novel 420 kDa

Protein Associated with the Presynaptic Cytomatrix." European Journal of Cell Biology. December 10, 1996. https://eurekamag.com/research/009/198/009198438.php.

Cesca, F., P. Baldelli, F. Valtorta, and F. Benfenati. 2010. "The Synapsins: Key Actors of Synapse Function and Plasticity." *Progress in Neurobiology* 91 (4): 313–48. https://doi.org/10.1016/j.pneurobio.2010.04.006.

Chen, Chun-Kan, Catherine Bregere, Jeremy Paluch, Jason F. Lu, Dion K. Dickman, and Karen T. Chang. 2014. "Activity-Dependent Facilitation of Synaptojanin and Synaptic Vesicle Recycling by the Minibrain Kinase." *Nature Communications* 5 (June): ncomms5246. https://doi.org/10.1038/ncomms5246.

Courcet, Jean-Benoît, Laurence Faivre, Perrine Malzac, Alice Masurel-Paulet, Estelle Lopez, Patrick Callier, Laetitia Lambert, et al. 2012. "The DYRK1A Gene Is a Cause of Syndromic Intellectual Disability with Severe Microcephaly and Epilepsy." *Journal of Medical Genetics* 49 (12): 731–36. https://doi.org/10.1136/jmedgenet-2012-101251.

Coutadeur, Séverine, Hélène Benyamine, Laurence Delalonde, Catherine de Oliveira, Bertrand Leblond, Alicia Foucourt, Thierry Besson, et al. 2015. "A Novel DYRK1A (Dual Specificity Tyrosine Phosphorylation-Regulated Kinase 1A) Inhibitor for the Treatment of Alzheimer's Disease: Effect on Tau and Amyloid Pathologies in Vitro." *Journal of Neurochemistry* 133 (3): 440–51. https://doi.org/10.1111/jnc.13018.

Debdab, Mansour, François Carreaux, Steven Renault, Meera Soundararajan, Oleg Fedorov, Panagis Filippakopoulos, Olivier Lozach, et al. 2011. "Leucettines, a Class of Potent Inhibitors of cdc2-Like Kinases and Dual Specificity, Tyrosine Phosphorylation Regulated Kinases Derived from the Marine Sponge Leucettamine B: Modulation of Alternative Pre-RNA Splicing." *Journal of Medicinal Chemistry* 54 (12): 4172–86. https://doi.org/10.1021/jm200274d.

Di Vona, Chiara, Daniela Bezdan, Abul B. M. M. K. Islam, Eulàlia Salichs, Nuria López-Bigas, Stephan Ossowski, and Susana de la Luna. 2015. "Chromatin-Wide Profiling of DYRK1A Reveals a Role as a Gene-Specific RNA Polymerase II CTD Kinase." *Molecular Cell* 57 (3): 506–20. https://doi.org/10.1016/j.molcel.2014.12.026.

Duchon, Arnaud, and Yann Herault. 2016. "DYRK1A, a Dosage-Sensitive Gene Involved in Neurodevelopmental Disorders, Is a Target for Drug Development in Down Syndrome." *Frontiers in Behavioral Neuroscience* 10. https://doi.org/10.3389/fnbeh.2016.00104.

Duchon, Arnaud, Matthieu Raveau, Claire Chevalier, Valérie Nalesso, Andrew J. Sharp, and Yann Herault. 2011. "Identification of the Translocation Breakpoints in the Ts65Dn and Ts1Cje Mouse Lines: Relevance for Modeling down Syndrome." *Mammalian Genome* 22 (11–12): 674. https://doi.org/10.1007/s00335-011-9356-0.

Ennaceur, A., and J. Delacour. 1988. "A New One-Trial Test for Neurobiological Studies of Memory in Rats. 1: Behavioral Data." *Behavioural Brain Research* 31 (1): 47–59. https://doi.org/10.1016/0166-4328(88)90157-X.

Fassio, Anna, Lysanne Patry, Sonia Congia, Franco Onofri, Amelie Piton, Julie Gauthier, Davide Pozzi, et al. 2011. "SYN1 Loss-of-Function Mutations in Autism and Partial Epilepsy Cause Impaired Synaptic Function." *Human Molecular Genetics* 20 (12): 2297–2307. https://doi.org/10.1093/hmg/ddr122.

Fenster, Steven D., Michael M. Kessels, Britta Qualmann, Wook J. Chung, Joanne Nash, Eckart D. Gundelfinger, and Craig C. Garner. 2003. "Interactions between Piccolo and the Actin/Dynamin-Binding Protein Abp1 Link Vesicle Endocytosis to Presynaptic Active Zones." *Journal of Biological Chemistry* 278 (22): 20268–77. https://doi.org/10.1074/jbc.M210792200.

Freund, Tamás F., István Katona, and Daniele Piomelli. 2003. "Role of Endogenous Cannabinoids in Synaptic Signaling." *Physiological Reviews* 83 (3): 1017–66. https://doi.org/10.1152/physrev.00004.2003.

Garcia, C. C., H. J. Blair, M. Seager, A. Coulthard, S. Tennant, M. Buddles, A. Curtis, and J. A. Goodship. 2004. "Identification of a Mutation in Synapsin I, a Synaptic Vesicle Protein, in a Family with Epilepsy." *Journal of Medical Genetics* 41 (3): 183–86. https://doi.org/10.1136/jmg.2003.013680.

García-Cerro, Susana, Paula Martínez, Verónica Vidal, Andrea Corrales, Jesús Flórez, Rebeca Vidal, Noemí Rueda, María L. Arbonés, and Carmen Martínez-Cué. 2014. "Overexpression of Dyrk1A Is Implicated in Several Cognitive, Electrophysiological and Neuromorphological Alterations Found in a Mouse Model of Down Syndrome." *PLOS ONE* 9 (9): e106572. https://doi.org/10.1371/journal.pone.0106572.

Garner, Craig C, Stefan Kindler, and Eckart D Gundelfinger. 2000. "Molecular Determinants of Presynaptic Active Zones." *Current Opinion in Neurobiology* 10 (3): 321–27. https://doi.org/10.1016/S0959-4388(00)00093-3.

Graaf, Katrin de, Paul Hekerman, Oliver Spelten, Andreas Herrmann, Len C. Packman, Konrad Büssow, Gerhard Müller-Newen, and Walter Becker. 2004. "Characterization of Cyclin L2, a Novel Cyclin with an Arginine/Serine-Rich Domain PHOSPHORYLATION BY DYRK1A AND COLOCALIZATION WITH SPLICING FACTORS." *Journal of Biological Chemistry* 279 (6): 4612–24. https://doi.org/10.1074/jbc.M310794200.

Grau, Cristina, Krisztina Arató, José M. Fernández-Fernández, Aitana Valderrama, Carlos Sindreu, Cristina Fillat, Isidre Ferrer, Susana de la Luna, and Xavier Altafaj. 2014. "DYRK1A-Mediated Phosphorylation of GluN2A at Ser1048 Regulates the Surface Expression and Channel Activity of GluN1/GluN2A Receptors." *Frontiers in Cellular Neuroscience* 8. https://doi.org/10.3389/fncel.2014.00331.

Guedj, Fayçal, Patricia Lopes Pereira, Sonia Najas, Maria-Jose Barallobre, Caroline Chabert, Benoit Souchet, Catherine Sebrie, et al. 2012. "DYRK1A: A Master Regulatory Protein Controlling Brain Growth." *Neurobiology of Disease* 46 (1): 190–203. https://doi.org/10.1016/j.nbd.2012.01.007.

Guedj, Fayçal, Catherine Sébrié, Isabelle Rivals, Aurelie Ledru, Evelyne Paly, Jean C. Bizot, Desmond Smith, et al. 2009. "Green Tea Polyphenols Rescue of Brain Defects Induced by Overexpression of DYRK1A." *PLOS ONE* 4 (2): e4606. https://doi.org/10.1371/journal.pone.0004606.

Gupta, Meenal, A. Ranjitha Dhanasekaran, and Katheleen J. Gardiner. 2016. "Mouse Models of Down Syndrome: Gene Content and Consequences." *Mammalian Genome* 27 (11–12): 538–55. https://doi.org/10.1007/s00335-016-9661-8.

Hawellek, David J., Joerg F. Hipp, Christopher M. Lewis, Maurizio Corbetta, and Andreas K. Engel. 2011. "Increased Functional Connectivity Indicates the Severity of Cognitive Impairment in Multiple Sclerosis." *Proceedings of the National Academy of Sciences* 108 (47): 19066–71. https://doi.org/10.1073/pnas.1110024108.

Head, Elizabeth, David Powell, Brian T. Gold, and Frederick A. Schmitt. 2012. "Alzheimer's Disease in Down Syndrome." *European Journal of Neurodegenerative Disease* 1 (3): 353–64.

Head, Elizabeth, Wayne Silverman, David Patterson, and Ira T. Lott. 2012. "Aging and Down Syndrome." Research article. Current Gerontology and Geriatrics Research. 2012. https://doi.org/10.1155/2012/412536.

Hilfiker, Sabine, Fabio Benfenati, Frédéric Doussau, Angus C. Nairn, Andrew J. Czernik, George J. Augustine, and Paul Greengard. 2005. "Structural Domains Involved in the Regulation of Transmitter Release by Synapsins." *Journal of Neuroscience* 25 (10): 2658–69. https://doi.org/10.1523/JNEUROSCI.4278-04.2005.

Himpel, Sunke, Werner Tegge, Ronald Frank, Susanne Leder, Hans-Georg Joost, and Walter Becker. 2000. "Specificity Determinants of Substrate Recognition by the Protein

Kinase DYRK1A." *Journal of Biological Chemistry* 275 (4): 2431–38. https://doi.org/10.1074/jbc.275.4.2431.

Hübner, Neele S., Anna E. Mechling, Hsu-Lei Lee, Marco Reisert, Thomas Bienert, Jürgen Hennig, Dominik von Elverfeldt, and Laura-Adela Harsan. 2017. "The Connectomics of Brain Demyelination: Functional and Structural Patterns in the Cuprizone Mouse Model." *NeuroImage* 146 (February): 1–18. https://doi.org/10.1016/j.neuroimage.2016.11.008.

Jiang, Xiaoling, Chunhong Liu, Tao Yu, Li Zhang, Kai Meng, Zhuo Xing, Pavel V. Belichenko, et al. 2015. "Genetic Dissection of the Down Syndrome Critical Region." *Human Molecular Genetics* 24 (22): 6540–51. https://doi.org/10.1093/hmg/ddv364.

Jin, Nana, Xiaomin Yin, Jianlan Gu, Xinhua Zhang, Jianhua Shi, Wei Qian, Yuhua Ji, et al. 2015. "Truncation and Activation of Dual Specificity Tyrosine Phosphorylation-Regulated Kinase 1A by Calpain I." *The Journal of Biological Chemistry* 290 (24): 15219–37. https://doi.org/10.1074/jbc.M115.645507.

Karp, Natasha A., Terry F. Meehan, Hugh Morgan, Jeremy C. Mason, Andrew Blake, Natalja Kurbatova, Damian Smedley, et al. 2015. "Applying the ARRIVE Guidelines to an In Vivo Database." *PLOS Biology* 13 (5): e1002151. https://doi.org/10.1371/journal.pbio.1002151.

Khan, Naghma, Farrukh Afaq, Mohammad Saleem, Nihal Ahmad, and Hasan Mukhtar. 2006. "Targeting Multiple Signaling Pathways by Green Tea Polyphenol (−)-Epigallocatechin-3-Gallate." *Cancer Research* 66 (5): 2500–2505. https://doi.org/10.1158/0008-5472.CAN-05-3636.

Kilkenny, Carol, William J. Browne, Innes C. Cuthill, Michael Emerson, and Douglas G. Altman. 2010. "Improving Bioscience Research Reporting: The ARRIVE Guidelines for Reporting Animal Research." *PLoS Biology* 8 (6). https://doi.org/10.1371/journal.pbio.1000412.

Kim, Hyeongki, Kyu-Sun Lee, Ae-Kyeong Kim, Miri Choi, Kwangman Choi, Mingu Kang, Seung-Wook Chi, et al. 2016. "A Chemical with Proven Clinical Safety Rescues Down-Syndrome-Related Phenotypes in through DYRK1A Inhibition." *Disease Models & Mechanisms* 9 (8): 839–48. https://doi.org/10.1242/dmm.025668.

Kimura, Ryo, Kouzin Kamino, Mitsuko Yamamoto, Aidaralieva Nuripa, Tomoyuki Kida, Hiroaki Kazui, Ryota Hashimoto, et al. 2007. "The DYRK1A Gene, Encoded in Chromosome 21 Down Syndrome Critical Region, Bridges between β-Amyloid Production and Tau Phosphorylation in Alzheimer Disease." *Human Molecular Genetics* 16 (1): 15–23. https://doi.org/10.1093/hmg/ddl437.

Korte, G., A. Dreiseitel, P. Schreier, A. Oehme, S. Locher, S. Geiger, J. Heilmann, and P. G. Sand. 2010. "Tea Catechins' Affinity for Human Cannabinoid Receptors." *Phytomedicine* 17 (1): 19–22. https://doi.org/10.1016/j.phymed.2009.10.001.

Leal-Ortiz, Sergio, Clarissa L. Waites, Ryan Terry-Lorenzo, Pedro Zamorano, Eckart D. Gundelfinger, and Craig C. Garner. 2008. "Piccolo Modulation of Synapsin1a Dynamics Regulates Synaptic Vesicle Exocytosis." *The Journal of Cell Biology* 181 (5): 831. https://doi.org/10.1083/jcb.200711167.

Li, Zhongyou, Tao Yu, Masae Morishima, Annie Pao, Jeffrey LaDuca, Jeffrey Conroy, Norma Nowak, Sei-Ichi Matsui, Isao Shiraishi, and Y. Eugene Yu. 2007. "Duplication of the Entire 22.9 Mb Human Chromosome 21 Syntenic Region on Mouse Chromosome 16 Causes Cardiovascular and Gastrointestinal Abnormalities." *Human Molecular Genetics* 16 (11): 1359–66. https://doi.org/10.1093/hmg/ddm086.

Litovchick, Larisa, Laurence A. Florens, Selene K. Swanson, Michael P. Washburn, and James A. DeCaprio. 2011. "DYRK1A Protein Kinase Promotes Quiescence and Senescence through DREAM Complex Assembly." *Genes & Development* 25 (8): 801–13. https://doi.org/10.1101/gad.2034211.

Llinás, R., J. A. Gruner, M. Sugimori, T. L. McGuinness, and P. Greengard. 1991. "Regulation by Synapsin I and Ca(2+)-Calmodulin-Dependent Protein Kinase II of the Transmitter Release in Squid Giant Synapse." *The Journal of Physiology* 436 (May): 257.

Llinás, R., T. L. McGuinness, C. S. Leonard, M. Sugimori, and P. Greengard. 1985. "Intraterminal Injection of Synapsin I or Calcium/Calmodulin-Dependent Protein Kinase II Alters Neurotransmitter Release at the Squid Giant Synapse." *Proceedings of the National Academy of Sciences of the United States of America* 82 (9): 3035.

Mao, Junhao, Peter Maye, Priit Kogerman, Francisco J. Tejedor, Rune Toftgard, Wei Xie, Guanqing Wu, and Dianqing Wu. 2002. "Regulation of Gli1 Transcriptional Activity in the Nucleus by Dyrk1." *Journal of Biological Chemistry* 277 (38): 35156–61. https://doi.org/10.1074/jbc.M206743200.

Marchal, Jan Pieter, Heleen Maurice-Stam, Bregje A. Houtzager, Susanne L. Rutgers van Rozenburg-Marres, Kim J. Oostrom, Martha A. Grootenhuis, and A. S. Paul van Trotsenburg. 2016. "Growing up with Down Syndrome: Development from 6 Months to 10.7 Years." *Research in Developmental Disabilities* 59 (December): 437–50. https://doi.org/10.1016/j.ridd.2016.09.019.

Martí, Eulàlia, Xavier Altafaj, Mara Dierssen, Susana de la Luna, Vassiliki Fotaki, Mónica Alvarez, Mercè Pérez-Riba, Isidro Ferrer, and Xavier Estivill. 2003. "Dyrk1A Expression Pattern Supports Specific Roles of This Kinase in the Adult Central Nervous System." *Brain Research* 964 (2): 250–63. https://doi.org/10.1016/S0006-8993(02)04069-6.

Martínez de Lagrán, M, X Altafaj, X Gallego, E Martí, X Estivill, I Sahún, C Fillat, and M Dierssen. 2004. "Motor Phenotypic Alterations in TgDyrk1a Transgenic Mice Implicate DYRK1A in Down Syndrome Motor Dysfunction." *Neurobiology of Disease* 15 (1): 132–42. https://doi.org/10.1016/j.nbd.2003.10.002.

Møller, Rikke S., Sabine Kübart, Maria Hoeltzenbein, Babett Heye, Ida Vogel, Christian P. Hansen, Corinna Menzel, et al. 2008. "Truncation of the Down Syndrome Candidate Gene DYRK1A in Two Unrelated Patients with Microcephaly." *The American Journal of Human Genetics* 82 (5): 1165–70. https://doi.org/10.1016/j.ajhg.2008.03.001.

Morris, A. F., Susan E. Vaughan, and P. Vaccaro. 1982. "MEASUREMENTS OF NEUROMUSCULAR TONE AND STRENGTH IN DOWN'S SYNDROME CHILDREN." *Journal of Intellectual Disability Research* 26 (1): 41–46. https://doi.org/10.1111/j.1365-2788.1982.tb00127.x.

Murakami, Noriko, David C. Bolton, Elizabeth Kida, Wen Xie, and Yu-Wen Hwang. 2012. "Phosphorylation by Dyrk1A of Clathrin Coated Vesicle-Associated Proteins: Identification of the Substrate Proteins and the Effects of Phosphorylation." *PLOS ONE* 7 (4): e34845. https://doi.org/10.1371/journal.pone.0034845.

Naert, Gaëlle, Valentine Ferré, Johann Meunier, Emeline Keller, Susanna Malmström, Laurent Givalois, François Carreaux, Jean-Pierre Bazureau, and Tangui Maurice. 2015. "Leucettine L41, a DYRK1A-Preferential DYRKs/CLKs Inhibitor, Prevents Memory Impairments and Neurotoxicity Induced by Oligomeric Aβ25–35 Peptide Administration in Mice." *European Neuropsychopharmacology* 25 (11): 2170–82. https://doi.org/10.1016/j.euroneuro.2015.03.018.

Nakano-Kobayashi, Akiko, Tomonari Awaya, Isao Kii, Yuto Sumida, Yukiko Okuno, Suguru Yoshida, Tomoe Sumida, Haruhisa Inoue, Takamitsu Hosoya, and Masatoshi Hagiwara. 2017. "Prenatal Neurogenesis Induction Therapy Normalizes Brain Structure and Function in Down Syndrome Mice." *Proceedings of the National Academy of Sciences* 114 (38): 10268–73. https://doi.org/10.1073/pnas.1704143114.

Nguyen, Thu Lan, Corinne Fruit, Yann Hérault, Laurent Meijer, and Thierry Besson. 2017. "Dual-Specificity Tyrosine Phosphorylation-Regulated Kinase 1A (DYRK1A)

Inhibitors: A Survey of Recent Patent Literature." *Expert Opinion on Therapeutic Patents* 27 (11): 1183–99. https://doi.org/10.1080/13543776.2017.1360285.

Nie, Xingju, Eric D. Hamlett, Ann-Charlotte Granholm, Edward S. Hui, Joseph A. Helpern, Jens H. Jensen, Heather A. Boger, Heather R. Collins, and Maria F. Falangola. 2015. "Evidence of Altered Age-Related Brain Cytoarchitecture in Mouse Models of down Syndrome: A Diffusional Kurtosis Imaging Study." *Magnetic Resonance Imaging* 33 (4): 437–47. https://doi.org/10.1016/j.mri.2014.12.008.

Oegema, R., A. de Klein, A. J. Verkerk, R. Schot, B. Dumee, H. Douben, B. Eussen, et al. 2010. "Distinctive Phenotypic Abnormalities Associated with Submicroscopic 21q22 Deletion Including DYRK1A." *Molecular Syndromology* 1 (3): 113. https://doi.org/10.1159/000320113.

Olmos-Serrano, J. Luis, William A. Tyler, Howard J. Cabral, and Tarik F. Haydar. 2016. "Longitudinal Measures of Cognition in the Ts65Dn Mouse: Refining Windows and Defining Modalities for Therapeutic Intervention in Down Syndrome." *Experimental Neurology* 279 (May): 40–56. https://doi.org/10.1016/j.expneurol.2016.02.005.

Ori-McKenney, Kassandra M., Richard J. McKenney, Hector H. Huang, Tun Li, Shan Meltzer, Lily Yeh Jan, Ronald D. Vale, Arun P. Wiita, and Yuh Nung Jan. 2016. "Phosphorylation of β-Tubulin by the Down Syndrome Kinase, Minibrain/DYRK1a, Regulates Microtubule Dynamics and Dendrite Morphogenesis." *Neuron* 90 (3): 551. https://doi.org/10.1016/j.neuron.2016.03.027.

Pons-Espinal, Meritxell, Maria Martinez de Lagran, and Mara Dierssen. 2013. "Environmental Enrichment Rescues DYRK1A Activity and Hippocampal Adult Neurogenesis in TgDyrk1A." *Neurobiology of Disease* 60 (December): 18–31. https://doi.org/10.1016/j.nbd.2013.08.008.

Powell, Nick M., Marc Modat, M. Jorge Cardoso, Da Ma, Holly E. Holmes, Yichao Yu, James O'Callaghan, et al. 2016. "Fully-Automated μMRI Morphometric Phenotyping of the Tc1 Mouse Model of Down Syndrome." *PLOS ONE* 11 (9): e0162974. https://doi.org/10.1371/journal.pone.0162974.

Pujol, Jesus, Laura del Hoyo, Laura Blanco-Hinojo, Susana de Sola, Dídac Macià, Gerard Martínez-Vilavella, Marta Amor, et al. 2015. "Anomalous Brain Functional Connectivity Contributing to Poor Adaptive Behavior in Down Syndrome." *Cortex* 64 (March): 148–56. https://doi.org/10.1016/j.cortex.2014.10.012.

Raichle, Marcus E. 2015a. "The Brain's Default Mode Network." *Annual Review of Neuroscience* 38 (1): 433–47. https://doi.org/10.1146/annurev-neuro-071013-014030.

———. 2015b. "The Brain's Default Mode Network." *Annual Review of Neuroscience* 38 (July): 433–47. https://doi.org/10.1146/annurev-neuro-071013-014030.

Reeves, Roger H., Nicholas G. Irving, Timothy H. Moran, Anny Wohn, Cheryl Kitt, Sangram S. Sisodia, Cecilia Schmidt, Roderick T. Bronson, and Muriel T. Davisson. 1995. "A Mouse Model for Down Syndrome Exhibits Learning and Behaviour Deficits." *Nature Genetics* 11 (2): 177–84. https://doi.org/10.1038/ng1095-177.

Roubertoux, Pierre L., Nathalie Baril, Pierre Cau, Christophe Scajola, Adeline Ghata, Catherine Bartoli, Patrice Bourgeois, Julie di Christofaro, Sylvie Tordjman, and Michèle Carlier. 2017. "Differential Brain, Cognitive and Motor Profiles Associated with Partial Trisomy. Modeling Down Syndrome in Mice." *Behavior Genetics* 47 (3): 305–22. https://doi.org/10.1007/s10519-017-9835-5.

Ryoo, Soo-Ryoon, Hyun-Jeong Cho, Hye-Won Lee, Hey Kyeong Jeong, Chinzorig Radnaabazar, Yeun-Soo Kim, Min-Jeong Kim, et al. 2008. "Dual-Specificity tyrosine(Y)-Phosphorylation Regulated Kinase 1A-Mediated Phosphorylation of Amyloid Precursor Protein: Evidence for a Functional Link between Down Syndrome and Alzheimer's Disease." *Journal of Neurochemistry* 104 (5): 1333–44. https://doi.org/10.1111/j.1471-4159.2007.05075.x.

Ryoo, Soo-Ryoon, Hey Kyeong Jeong, Chinzorig Radnaabazar, Jin-Ju Yoo, Hyun-Jeong Cho, Hye-Won Lee, In-Sook Kim, et al. 2007. "DYRK1A-Mediated Hyperphosphorylation of Tau A FUNCTIONAL LINK BETWEEN DOWN SYNDROME AND ALZHEIMER DISEASE." *Journal of Biological Chemistry* 282 (48): 34850–57. https://doi.org/10.1074/jbc.M707358200.

Ryu, Young Shin, So Young Park, Min-Su Jung, Song-Hee Yoon, Mi-Yang Kwen, Sun-Young Lee, Sun-Hee Choi, et al. 2010. "Dyrk1A-Mediated Phosphorylation of Presenilin 1: A Functional Link between Down Syndrome and Alzheimer's Disease." *Journal of Neurochemistry* 115 (3): 574–84. https://doi.org/10.1111/j.1471-4159.2010.06769.x.

Scales, Timothy M. E., Shen Lin, Michaela Kraus, Robert G. Goold, and Phillip R. Gordon-Weeks. 2009. "Nonprimed and DYRK1A-Primed GSK3β-Phosphorylation Sites on MAP1B Regulate Microtubule Dynamics in Growing Axons." *J Cell Sci* 122 (14): 2424–35. https://doi.org/10.1242/jcs.040162.

Sforazzini, Francesco, Adam J. Schwarz, Alberto Galbusera, Angelo Bifone, and Alessandro Gozzi. 2014. "Distributed BOLD and CBV-Weighted Resting-State Networks in the Mouse Brain." *NeuroImage* 87 (February): 403–15. https://doi.org/10.1016/j.neuroimage.2013.09.050.

Shi, Jianhua, Tianyi Zhang, Chunlei Zhou, Muhammad Omar Chohan, Xiaosong Gu, Jerzy Wegiel, Jianhua Zhou, et al. 2008. "Increased Dosage of Dyrk1A Alters Alternative Splicing Factor (ASF)-Regulated Alternative Splicing of Tau in Down Syndrome." *The Journal of Biological Chemistry* 283 (42): 28660–69. https://doi.org/10.1074/jbc.M802645200.

Sitz, J. H., K. Baumgärtel, B. Hämmerle, C. Papadopoulos, P. Hekerman, F. J. Tejedor, W. Becker, and B. Lutz. 2008. "The down Syndrome Candidate Dual-Specificity Tyrosine Phosphorylation-Regulated Kinase 1A Phosphorylates the Neurodegeneration-Related Septin 4." *Neuroscience* 157 (3): 596–605. https://doi.org/10.1016/j.neuroscience.2008.09.034.

Smith, Breland, Federico Medda, Vijay Gokhale, Travis Dunckley, and Christopher Hulme. 2012. "Recent Advances in the Design, Synthesis, and Biological Evaluation of Selective DYRK1A Inhibitors: A New Avenue for a Disease Modifying Treatment of Alzheimer's?" *ACS Chemical Neuroscience* 3 (11): 857–72. https://doi.org/10.1021/cn300094k.

Smith, Desmond J., Mary E. Stevens, Sharmila P. Sudanagunta, Roderick T. Bronson, Michael Makhinson, Ayako M. Watabe, Thomas J. O'Dell, et al. 1997. "Functional Screening of 2 Mb of Human Chromosome 21q22.2 in Transgenic Mice Implicates Minibrain in Learning Defects Associated with Down Syndrome." *Nature Genetics* 16 (1): 28–36. https://doi.org/10.1038/ng0597-28.

Soppa, Ulf, Julian Schumacher, Victoria Florencio Ortiz, Tobias Pasqualon, Francisco Tejedor, and Walter Becker. 2014. "The Down Syndrome-Related Protein Kinase DYRK1A Phosphorylates p27Kip1 and Cyclin D1 and Induces Cell Cycle Exit and Neuronal Differentiation." *Cell Cycle*, May. https://doi.org/10.4161/cc.29104.

Souchet, Benoit, Fayçal Guedj, Ignasi Sahún, Arnaud Duchon, Fabrice Daubigney, Anne Badel, Yuchio Yanagawa, et al. 2014. "Excitation/Inhibition Balance and Learning Are Modified by Dyrk1a Gene Dosage." *Neurobiology of Disease* 69 (September): 65–75. https://doi.org/10.1016/j.nbd.2014.04.016.

Souchet, Benoit, Alizée Latour, Yuchen Gu, Fabrice Daubigney, Jean-Louis Paul, Jean-Maurice Delabar, and Nathalie Janel. 2015. "Molecular Rescue of DYRK1A Overexpression in Cystathionine Beta Synthase-Deficient Mouse Brain by Enriched Environment Combined with Voluntary Exercise." *Journal of Molecular Neuroscience* 55 (2): 318–23. https://doi.org/10.1007/s12031-014-0324-5.

Stafford, James M., Benjamin R. Jarrett, Oscar Miranda-Dominguez, Brian D. Mills, Nicholas Cain, Stefan Mihalas, Garet P. Lahvis, et al. 2014. “Large-Scale Topology and the Default Mode Network in the Mouse Connectome.” *Proceedings of the National Academy of Sciences* 111 (52): 18745–50. https://doi.org/10.1073/pnas.1404346111.

Sureshbabu, Rengasamy, Rashmi Kumari, Subramaniam Ranugha, Ramanathan Sathyamoorthy, Carounanidy Udayashankar, and Paquirissamy Oudeacoumar. 2011. “Phenotypic and Dermatological Manifestations in Down Syndrome.” *Dermatology Online Journal* 17 (2). http://escholarship.org/uc/item/8jx5f2v2.

Tahtouh, Tania, Jonathan M. Elkins, Panagis Filippakopoulos, Meera Soundararajan, Guillaume Burgy, Emilie Durieu, Claude Cochet, et al. 2012. “Selectivity, Cocrystal Structures, and Neuroprotective Properties of Leucettines, a Family of Protein Kinase Inhibitors Derived from the Marine Sponge Alkaloid Leucettamine B.” Research-article. October 8, 2012. https://doi.org/10.1021/jm301034u.

Thomazeau, Aurore, Olivier Lassalle, Jillian Iafrati, Benoit Souchet, Fayçal Guedj, Nathalie Janel, Pascale Chavis, Jean Delabar, and Olivier J. Manzoni. 2014. “Prefrontal Deficits in a Murine Model Overexpressing the Down Syndrome Candidate Gene Dyrk1a.” *Journal of Neuroscience* 34 (4): 1138–47. https://doi.org/10.1523/JNEUROSCI.2852-13.2014.

Torre, Rafael de la, Susana de Sola, Gimena Hernandez, Magí Farré, Jesus Pujol, Joan Rodriguez, Josep María Espadaler, et al. 2016. “Safety and Efficacy of Cognitive Training plus Epigallocatechin-3-Gallate in Young Adults with Down’s Syndrome (TESDAD): A Double-Blind, Randomised, Placebo-Controlled, Phase 2 Trial.” *The Lancet Neurology* 15 (8): 801–10. https://doi.org/10.1016/S1474-4422(16)30034-5.

Torre, Rafael, Susana Sola, Meritxell Pons, Arnaud Duchon, María Martínez Lagran, Magí Farré, Montserrat Fitó, et al. 2014a. “Epigallocatechin-3-gallate, a DYRK1A Inhibitor, Rescues Cognitive Deficits in Down Syndrome Mouse Models and in Humans.” *Molecular Nutrition & Food Research* 58 (2): 278–88. https://doi.org/10.1002/mnfr.201300325.

———. 2014b. “Epigallocatechin-3-gallate, a DYRK1A Inhibitor, Rescues Cognitive Deficits in Down Syndrome Mouse Models and in Humans.” *Molecular Nutrition & Food Research* 58 (2): 278–88. https://doi.org/10.1002/mnfr.201300325.

Valetto, Angelo, Alessandro Orsini, Veronica Bertini, Benedetta Toschi, Alice Bonuccelli, Francesca Simi, Irene Sammartino, Grazia Taddeucci, Paolo Simi, and Giuseppe Saggese. 2012. “Molecular Cytogenetic Characterization of an Interstitial Deletion of Chromosome 21 (21q22.13q22.3) in a Patient with Dysmorphic Features, Intellectual Disability and Severe Generalized Epilepsy.” *European Journal of Medical Genetics*, Epilepsy and Genetics, 55 (5): 362–66. https://doi.org/10.1016/j.ejmg.2012.03.011.

Vega, Jennifer N., Timothy J. Hohman, Jennifer R. Pryweller, Elisabeth M. Dykens, and Tricia A. Thornton-Wells. 2015. “Resting-State Functional Connectivity in Individuals with Down Syndrome and Williams Syndrome Compared with Typically Developing Controls.” *Brain Connectivity* 5 (8): 461–75. https://doi.org/10.1089/brain.2014.0266.

Waites, Clarissa L., Sergio A. Leal-Ortiz, Till F. M. Andlauer, Stefan J. Sigrist, and Craig C. Garner. 2011. “Piccolo Regulates the Dynamic Assembly of Presynaptic F-Actin.” *The Journal of Neuroscience : The Official Journal of the Society for Neuroscience* 31 (40): 14250. https://doi.org/10.1523/JNEUROSCI.1835-11.2011.

Walte, Agnes, Katharina Rüben, Ruth Birner-Gruenberger, Christian Preisinger, Simone Bamberg-Lemper, Nikolaus Hilz, Franz Bracher, and Walter Becker. 2013. “Mechanism of Dual Specificity Kinase Activity of DYRK1A.” *FEBS Journal* 280 (18): 4495–4511. https://doi.org/10.1111/febs.12411.

Wegiel, Jerzy, Wojciech Kaczmarski, Madhabi Barua, Izabela Kuchna, Krzysztof Nowicki, Kuo-Chiang Wang, Jarek Wegiel, et al. 2011. “The Link Between DYRK1A

Overexpression and Several-Fold Enhancement of Neurofibrillary Degeneration with 3-Repeat Tau Protein in Down Syndrome." *Journal of Neuropathology and Experimental Neurology* 70 (1): 36–50. https://doi.org/10.1097/NEN.0b013e318202bfa1.

Wilson, Rachel I., and Roger A. Nicoll. 2002. "Endocannabinoid Signaling in the Brain." *Science* 296 (5568): 678–82. https://doi.org/10.1126/science.1063545.

Woods, Y L, P Cohen, W Becker, R Jakes, M Goedert, X Wang, and C G Proud. 2001. "The Kinase DYRK Phosphorylates Protein-Synthesis Initiation Factor eIF2Bepsilon at Ser539 and the Microtubule-Associated Protein Tau at Thr212: Potential Role for DYRK as a Glycogen Synthase Kinase 3-Priming Kinase." *Biochemical Journal* 355 (Pt 3): 609–15.

Yamamoto, Toshiyuki, Keiko Shimojima, Tsutomu Nishizawa, Mari Matsuo, Masahiro Ito, and Katsumi Imai. 2011. "Clinical Manifestations of the Deletion of Down Syndrome Critical Region Including DYRK1A and KCNJ6." *American Journal of Medical Genetics Part A* 155 (1): 113–19. https://doi.org/10.1002/ajmg.a.33735.

Yang, Chung S., Xin Wang, Gang Lu, and Sonia C. Picinich. 2009. "Cancer Prevention by Tea: Animal Studies, Molecular Mechanisms and Human Relevance." *Nature Reviews Cancer* 9 (6): 429–39. https://doi.org/10.1038/nrc2641.

Yu, Tao, Chunhong Liu, Pavel Belichenko, Steven J. Clapcote, Shaomin Li, Annie Pao, Alexander Kleschevnikov, et al. 2010. "Effects of Individual Segmental Trisomies of Human Chromosome 21 Syntenic Regions on Hippocampal Long-Term Potentiation and Cognitive Behaviors in Mice." *Brain Research* 1366 (December): 162–71. https://doi.org/10.1016/j.brainres.2010.09.107.

Zhou, Yuan, Karl J. Friston, Peter Zeidman, Jie Chen, Shu Li, and Adeel Razi. 2018. "The Hierarchical Organization of the Default, Dorsal Attention and Salience Networks in Adolescents and Young Adults." *Cerebral Cortex* 28 (2): 726–37. https://doi.org/10.1093/cercor/bhx307.

Yin X, Jin N, Gu J, Shi J, Zhou J, Gong CX, Iqbal K, Grundke-Iqbal I, Liu F. Dual-specificity tyrosine phosphorylation-regulated kinase 1A (Dyrk1A) modulates serine/arginine-rich protein 55 (SRp55)-promoted Tau exon 10 inclusion. J Biol Chem. 2012 287:30497-506. doi: 10.1074/jbc.M112.355412.

Figures

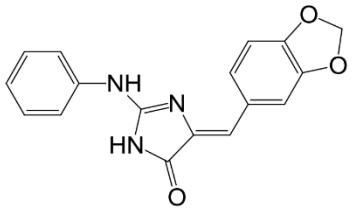

Leucettine **L41**

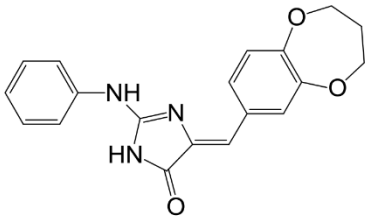

Leucettine **L43**

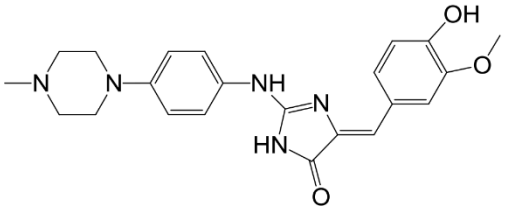

Leucettine **L99**

Kinase	L41	L43	L99
CDK1/cyclin B	>10	>10	>10
CDK2/cyclin A	>10	>10	>10
CDK5/p25	>10	>10	>10
CDK9/cyclin T	>10	>10	0.32
CK1	>10	>10	0.78
CLK1	0.023	>10	0.012
CLK2	0.130	-	0.030
CLK3	1.2	-	0.7
CLK4	0.023	>10	0.012
DYRK1A	0.024	7.4	0.014
DYRK1B	0.062	>10	0.020
DYRK2	0.014	>10	0.015
DYRK3	0.230	-	0.010
GSK3	0.6	-	0.2
CK2	0.510	-	-
PIM1	1.2	>10	0.21
CB1 arrestin	0.314	0.890	-

Figure 1. Chemical structure and selectivity of Leucettines used in this study. Selectivity of Leucettines L41, L43 and L99 was assessed *in vitro* on 16 recombinant kinases, and in a cellular CB1 annexin assay. Dose-response curves provided IC_{50} values (reported in µM). -, no inhibition at 10 µM.

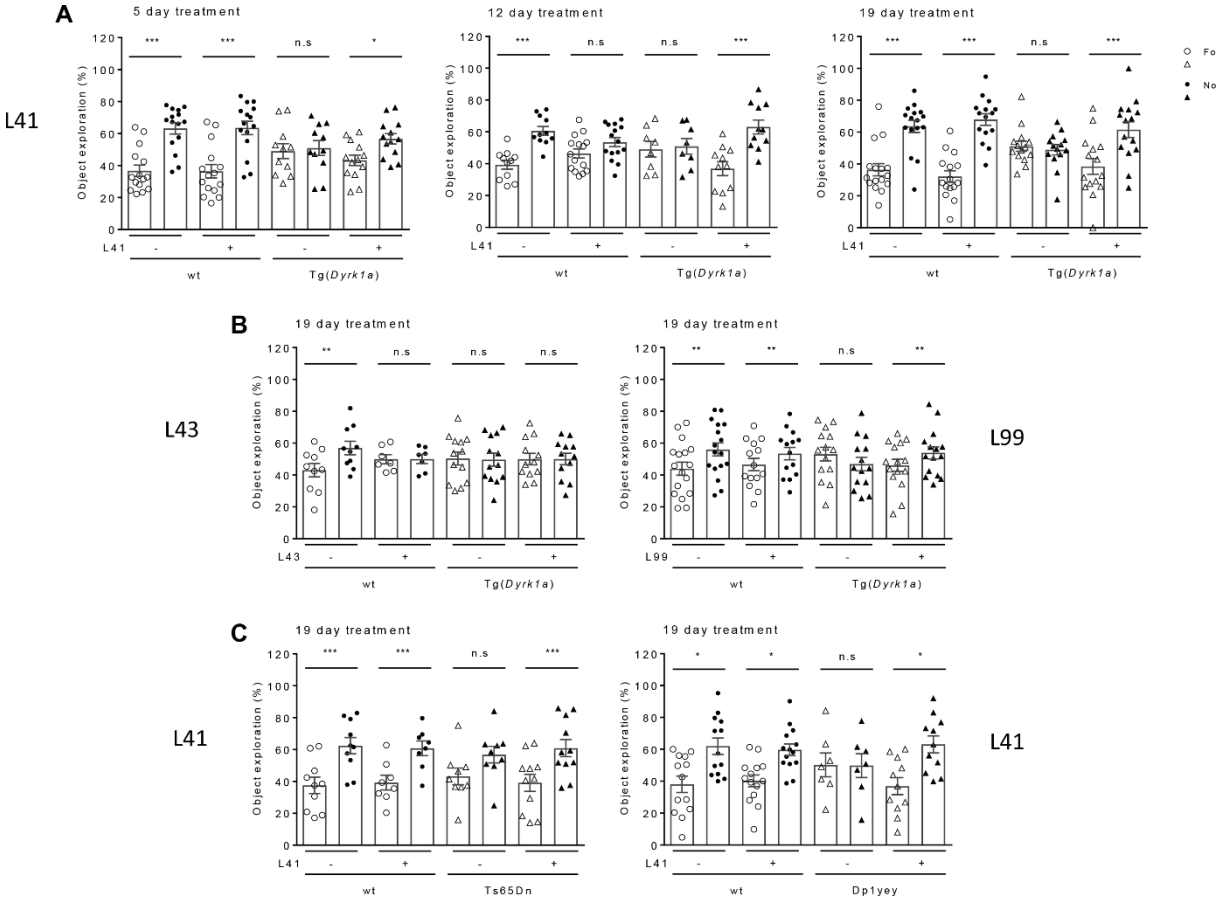

Figure 2. DYRK1a specific inhibitors rescue NOR deficits induced in Tg(*Dyrk1a*), Ts65Dn and Dp1yey trisomic mice. A. Duration of treatment. NOR test results for Tg(*Dyrk1a*) mice treated with L41 or vehicle for 5, 12 or 19 days. Percentage object exploration by sniffing was determined for each object after a 24 h retention delay (familiar object: open symbol; novel object: filled symbol). NOR results of three Tg(*Dyrk1a*) cohorts treated with L41 for 5 (left), 12 (center) or 19 (right) days. Tg(*Dyrk1a*) and Ts65Dn treated animals spent more time exploring the novel object compared to control mice, showing a rescue of their recognition memory. **Left**, 5 days treatment induced a NOR rescue in Tg(*Dyrk1a*) animals (wt: n=15, p<0.001; treated wt: n=15, p<0.001; untreated Tg(*Dyrk1a*): n=11, p=0.8; treated Tg(*Dyrk1a*): n=13, p=0.02). **Center**, a more consistent rescue was obtained after 12 days of L41 treatment (not treated wt: n=12, p<0.001; treated wt: n=15, p=0.11; untreated Tg(*Dyrk1a*) n=8, p=0.76; treated Tg(*Dyrk1a*): n=11, p<0.001). **Right**, rescue obtained after 19 days of L41 treatment: the exploration was significantly different for wt (n=15, p<0.001), treated wt (n=15, p<0.001), treated Tg(*Dyrk1a*)(n=15b, p<0.001) but not for non-treated transgenic (n=13, p=0.64). **B. Treatment with L43 (left) and L99 (right).** L99 treatment induced a cognitive rescue in the Tg(*Dyrk1a*) mice whereas L43 treatment had no effect. L99 (left): (wt: n=10, p=0.02; treated wt: n=12, p=0.003; Tg(*Dyrk1a*): n=12,

p=0.01; treated Tg(*Dyrk1a*): n=9 p<0.001); L43 (right): (wt n=12, p=0.008; treated wt: n=7, p=0.9; Tg(*Dyrk1a*): n=13, p=0.91; treated Tg(*Dyrk1a*): n=12, p=0.71). **C. Ts65Dn and Dp1yey models. Left**, In the Ts65Dn study, a significant statistical difference was observed for untreated wt (n=10 p<0.001), treated wt (n=8, p=0.009) and treated Ts65Dn (n=11, p=0.002) but not for untreated Ts65Dn animals (n=9, p=0.08). **Right**, L41 also normalizes the recognition memory of Dp1Yey mice (wt: n=13, p=0.04; treated wt: n=14, p=0.02; Dp1Yey: n=7, p=0.98; treated Dp1Yey: n=11, p=0.03). Data are represented as mean +/- s.e.m. with individual points per animal. Statistical analysis was performed with the two-way ANOVA test, Tukey post-hoc. n.s., not significant. *p<0.05, **p<0.01, ***p<0.001.

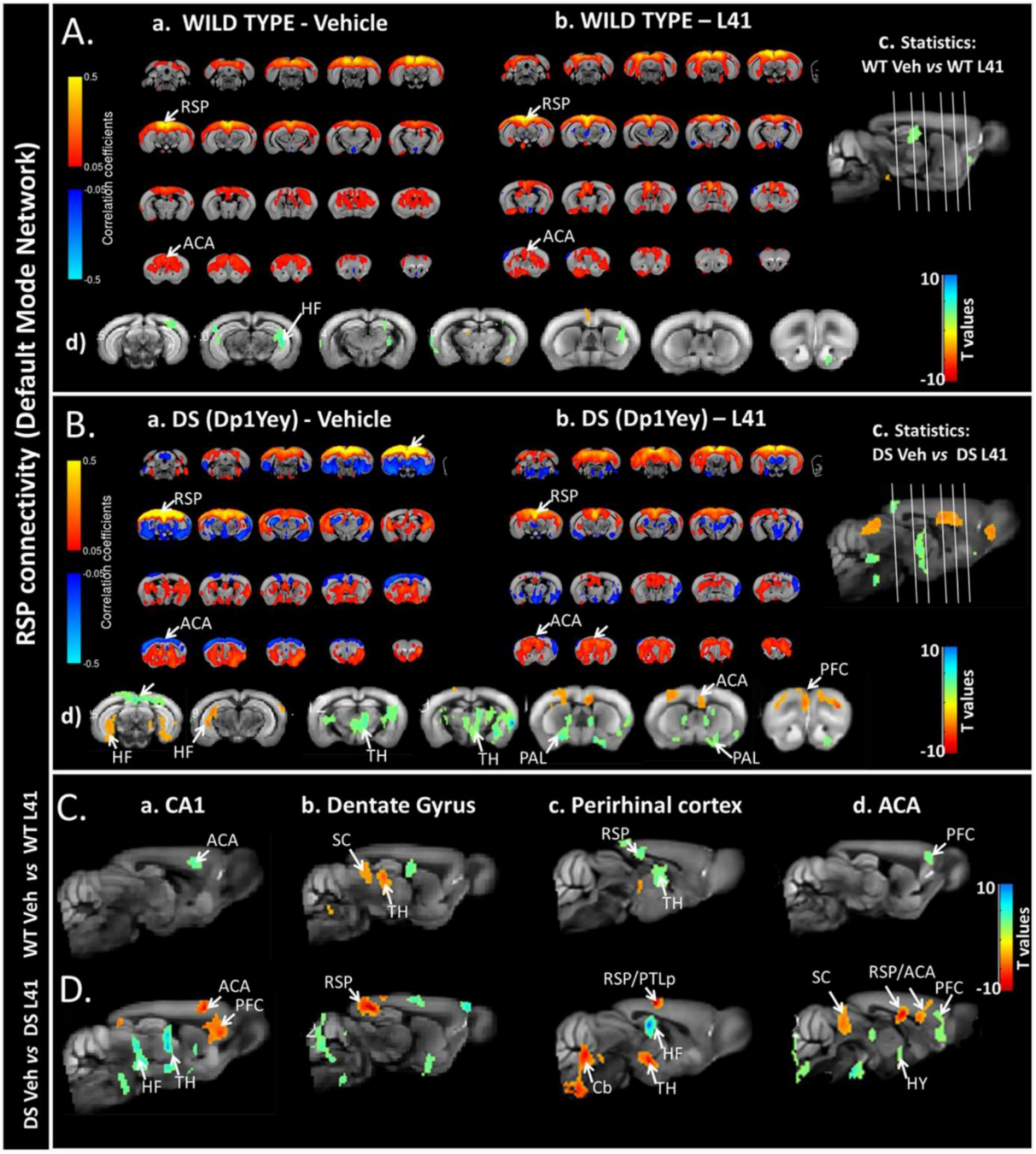

Figure 3. Influence of L41 on mouse brain functional connectivity (FC) patterns mapped via rsfMRI. A,B. Default mode network (DMN) pattern in wt (**a**) and Dp1Yey (**b**) animals, mapped using the retrosplenial (RSP) cortex (core hub of DMN) as seed region. **A-a** shows the typical DMN-like pattern observed in mice, spatially covering the middle rostro-caudal cortical axis of wt animals treated with vehicle, connecting RSP and rostro-medial anterior cingulate cortex. **A-b** L41 treatment in wt animals slightly modifies the DMN patterns compared to wt-Vehicle (see also statistics in **A-c**, sagittal view and **A-d**, coronal view; two-

tailed t-test, $p<0.01$). Red-orange scale quantifies the areas where L41 treatment results in increased FC of wt-L41 compared to wt-Vehicle. Blue-green scale indicates areas with decreased RSP connectivity after L41 treatment, compared with vehicle treated wt mice. **B-a** demonstrates strongly altered DMN network in Dp1Yey animals treated with vehicle compared to wt vehicle treated animals (**A-a**, wt-Vehicle), highlighting the pathological connectivity features of the mutant animals. **B-b**, L41 treatment in mutant Dp1Yey animals (DP16-L41) strongly modifies the DMN, restoring the positive correlations (red) of RSP cortex with the frontal brain areas (arrows, **B-b**). Voxel vise statistics shown in panel **B-c** and **B-d** indicate, in red-orange, the areas where L41 treatment results in increased functional connectivity of DP16-L41 group compared to DP16-Vehicle group. Blue-green scale indicates areas with decreased RSP connectivity after L41 treatment, compared with vehicle treated group mutant mice. In **A-a**, **A-b**, **B-a** and **B-b**, red indicates the positively correlated areas (0.1 to 0.5 correlation coefficients). Blue indicates negatively correlated areas (-0.1 to -0.5 correlation coefficients). **C, D** panels show statistically significant differences (two-tailed t-test, $p<0.01$) in the functional connectivity patterns after L41 treatment of wt (**C**) and Dp1Yey (**D**) animals. **C-a**, CA1 FC; **C-b**, dentate gyrus FC; **C-c**, perirhinal cortex FC; **C-d**, anterior cingulate cortex (ACC) FC. Red-orange shows the brain areas where L41 treatment results in increased FC while blue-green scale indicates areas with decreased connectivity after L41, compared with vehicle-treated mice (**C**, wt; **D**, Dp1Yey).

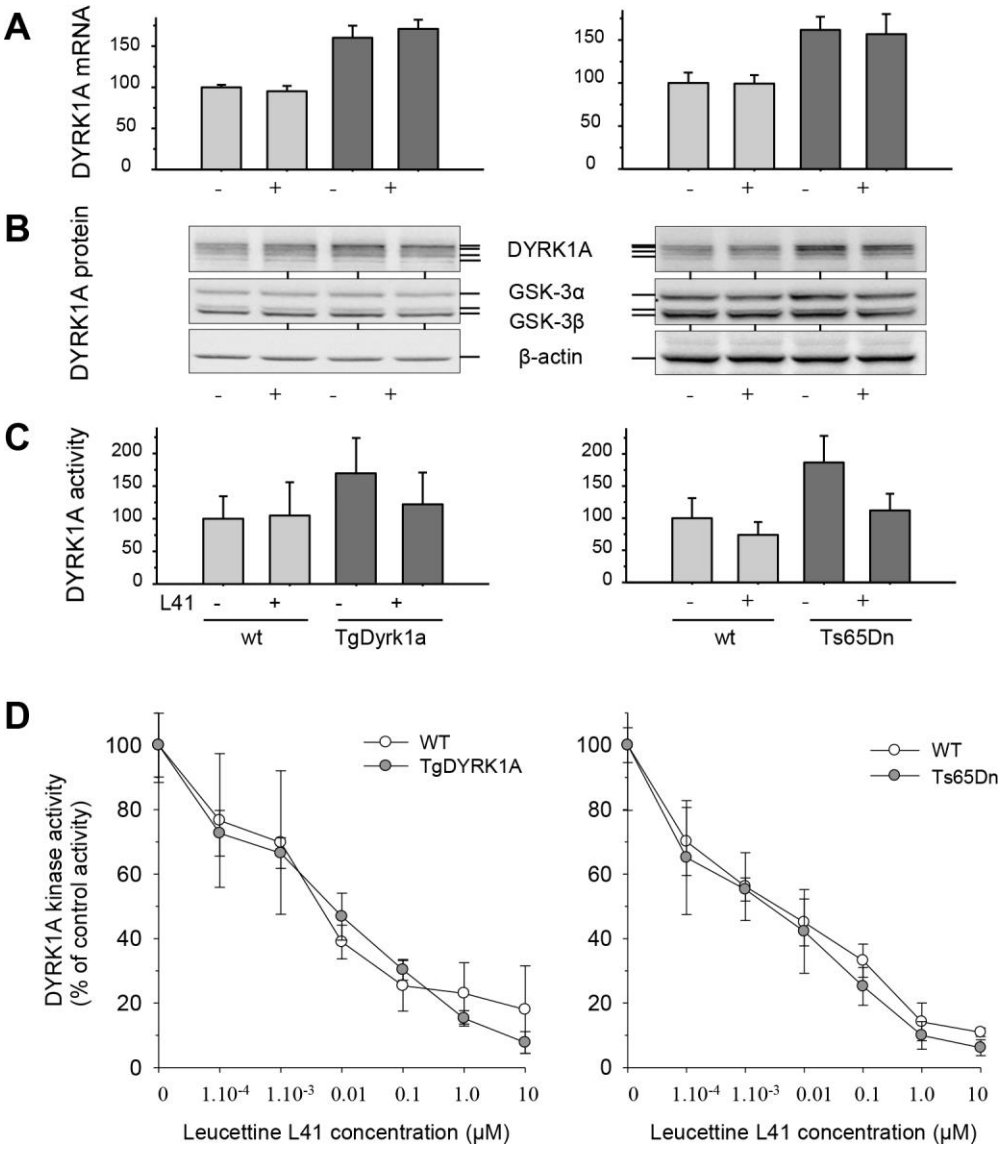

Figure 4. DYRK1A mRNA (A) and protein (B) expression, and catalytic activity (C) in Tg(*Dyrk1a*) and corresponding wt mice brains (left) and in Ts65Dn and corresponding wt mice brains (right). A. mRNA expression. Total RNA was extracted, purified and reverse transcribed into cDNA. mRNA expression of DYRK1A, GSK-3β and reference RPLPO was quantified by qPCR from the amplification of cDNA with specific primers (one primer annealing to an exon-exon junction). Results are presented as mean ± s.e. of 4-6 measurements and are shown relative to RPLP0 expression, normalized on wt GSK-3β expression. **B. protein expression.** Total proteins were extracted, resolved on SDS-PAGE and analyzed by WB using antibodies directed against DYRK1A, GSK-3α/β and actin (loading control). **C. DYRK1A catalytic activity.** DYRK1A was purified from brain extracts by immunoprecipitation and GSK-3 was purified by affinity chromatography on axin-agarose

beads. Activities of the purified kinases were assayed in triplicate in a radioactive kinase assay using specific peptide substrates and are reported after normalization with wt GSK-3 activities (mean ± s.e.). **D. In vitro DYRK1A kinase activity.** The catalytic activity of DYRK1A immunoprecipitated from brains of Tg(*Dyrk1a*) and Ts65Dn mice and their respective controls was assayed in the presence of a range of L41 concentrations.

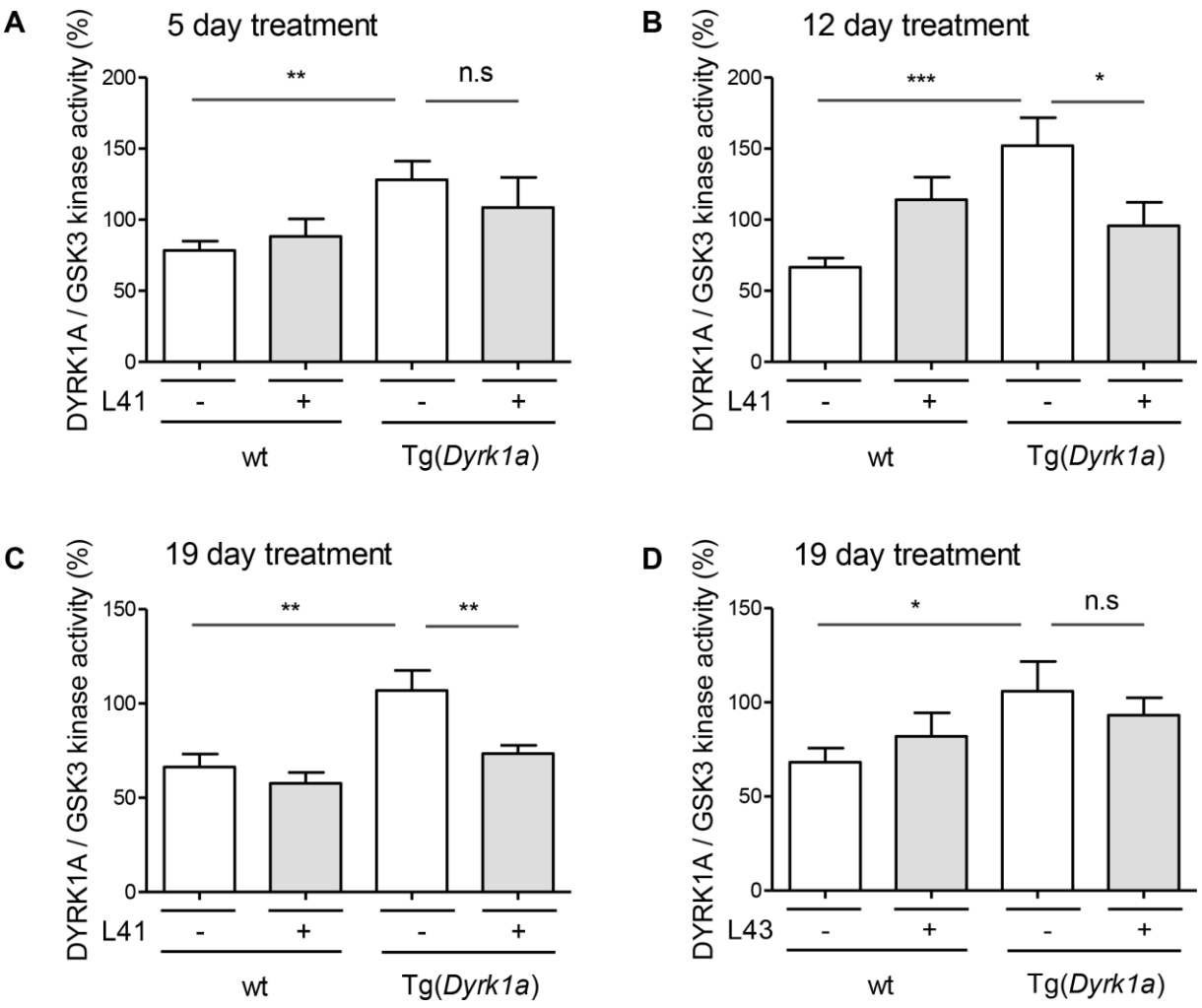

Figure 5. Effect on L41 treatment duration (A-C) and treatment with L43 (D). Wt and Tg(*Dyrk1a*) mice were treated with L41 or vehicle for 5 (**A**), 12 (**B**) or 19 (**C**) days or L43 or vehicle for 19 (**D**) days. Brains were recovered and extracted, DYRK1A and GSK-3 were immunopurified and affinity-purified, respectively, and assayed for their catalytic activities. DYRK1A kinase activity was normalized with GSK-3 activities in each extract (mean $\pm$ s.e.). DYRK1A inhibition in Tg(*Dyrk1a*) mice brains was not significant after a 5 day treatment ($p=0.42$), but was increasingly significant after 12 ($p=0.04$) and 19 ($p=0.01$) days of L41 treatment. 19 days treatment with kinase inactive L43 did not reduce DYRK1A activity in Tg(*Dyrk1a*) mice ($p=0.5$).

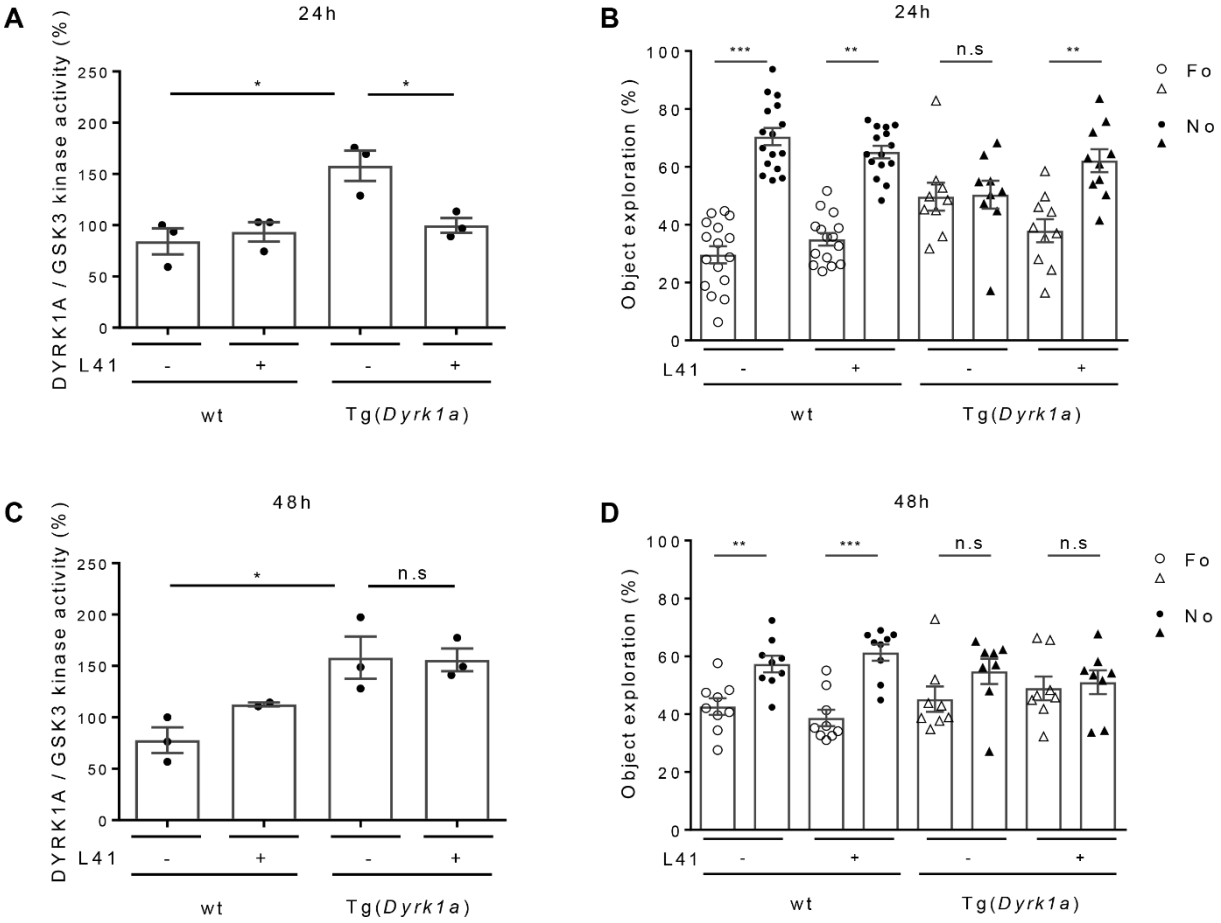

Figure 6. Persistence of the L41 inhibitory effect on DYRK1A activity (A, C) and rescue of NOR deficit (B, D). DYRK1A and GSK-3 activities were measured after purification from brains of wt (n=3), L41-treated wt (n=3), Tg(*Dyrk1a*) (n=3) and L41-treated Tg(*Dyrk1a*) (n=3) animals, 24 h (**A**) or 48 h (**C**) following the end of a 19 day L41 treatment. After 24 h (p=0.02), but not at 48 h (p=0.93), the DYRK1A catalytic activity of the treated Tg(*Dyrk1a*) mice brain was normalized compared to that of non-treated animals. NOR tests were performed either 24 h (**B**) or 48 h (**D**) after the last day of the 19 day L41 treatment. Although the rescuing effect was detectable 24 h after the last L41 treatment (p=0.01), no rescue was seen after a 48 h delay (p=0.72).

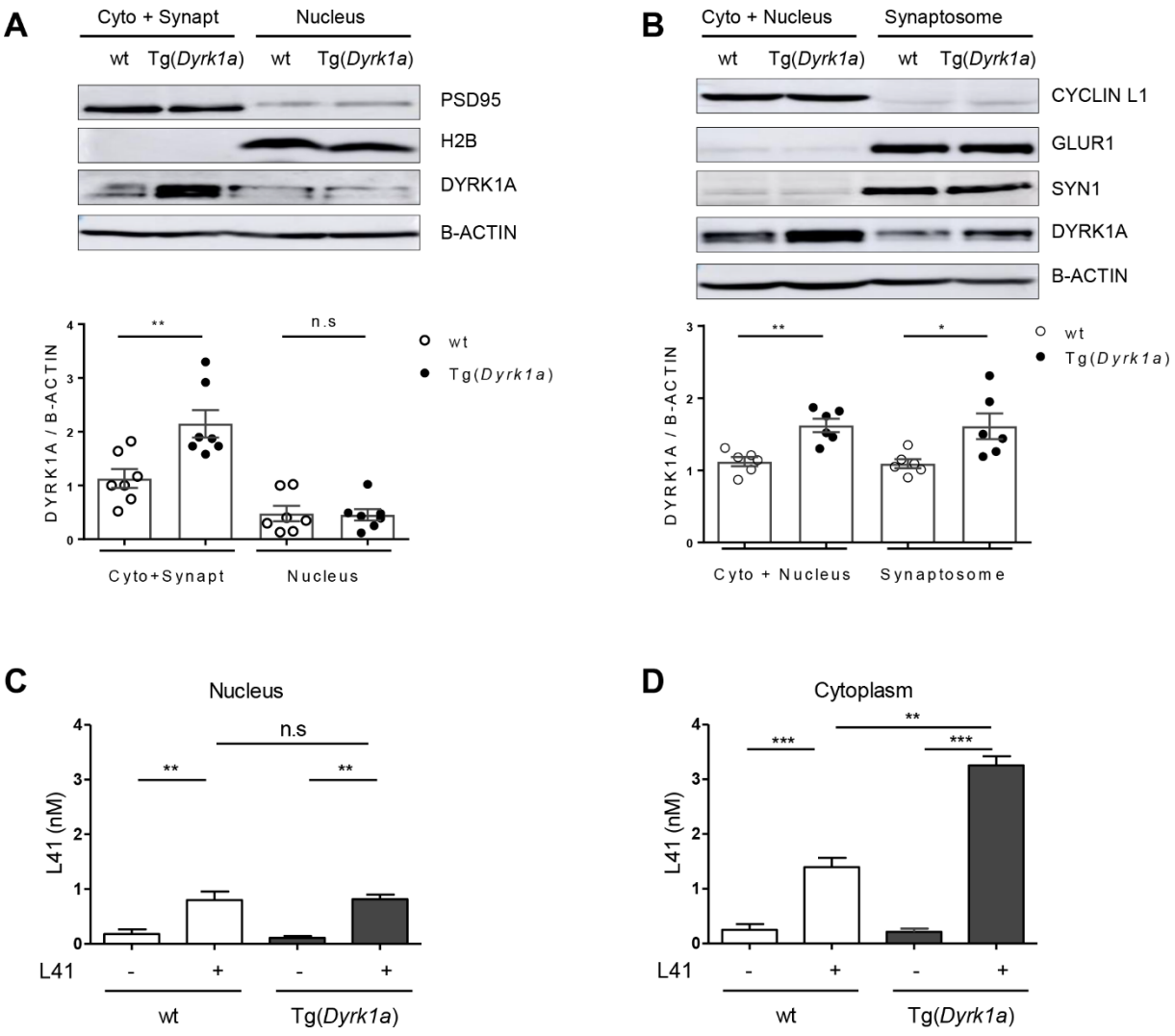

Figure 7. DYRK1A (A, B) and L41 (C, D) subcellular localization. A, B. Wt or Tg(*Dyrk1a*) brains were fractionated by two methods and the expression of DYRKA was estimated by WB following SDS-PAGE. Reference sub-compartment specific proteins were detected by WB. **A.** DYRK1A expression in cytoplasm + synaptosomes and in nuclear fractions (wt n=6; Tg(*Dyrk1a*) n=6). DYRK1A overexpression is observed in the cytoplasm + synaptosomes fraction (p=0.006), but not in the nuclear fraction (p=0.9). WB of specific markers validate the purity of fractions: PSD95 (95 kDa, cytoplasmic + synaptosomal marker), H2B (17 kDa, nuclear marker), b-Actin (42 kDa, housekeeping protein). **B.** DYRK1A expression in cytoplasm + nuclei and in synaptosomal fractions (wt n=7; Tg(*Dyrk1a*) n=7). DYRK1A was overexpressed in both cytoplasmic + nuclear (p = 0.001) and synaptosomal (p=0.02) fractions. Fractionation is confirmed by WB of specific compartment markers: cyclin L1 (55 kDa, cytoplasmic + nuclear marker), GLUR1 (100 kDa, postsynaptic marker), SYN1 (74 kDa, presynaptic marker), b-Actin (42 kDa, housekeeping

protein). **C, D.** L41 subcellular levels. L41 in L41-treated wt (n=5) and Tg(*Dyrk1a*) (n=2) mice was well detected in the brain nuclear (**C**) and cytoplasmic (**D**) compartments compared to non-treated wt (n=5) and non-treated Tg(*Dyrk1a*) (n=5) mice. L41 distribution is not significantly different between the brain nuclear fractions of treated wt and Tg mice. In contrast L41 level is increased in the cytoplasm of treated Tg mice brain compared to the cytoplasm of control wt mice brain (p=0.002).

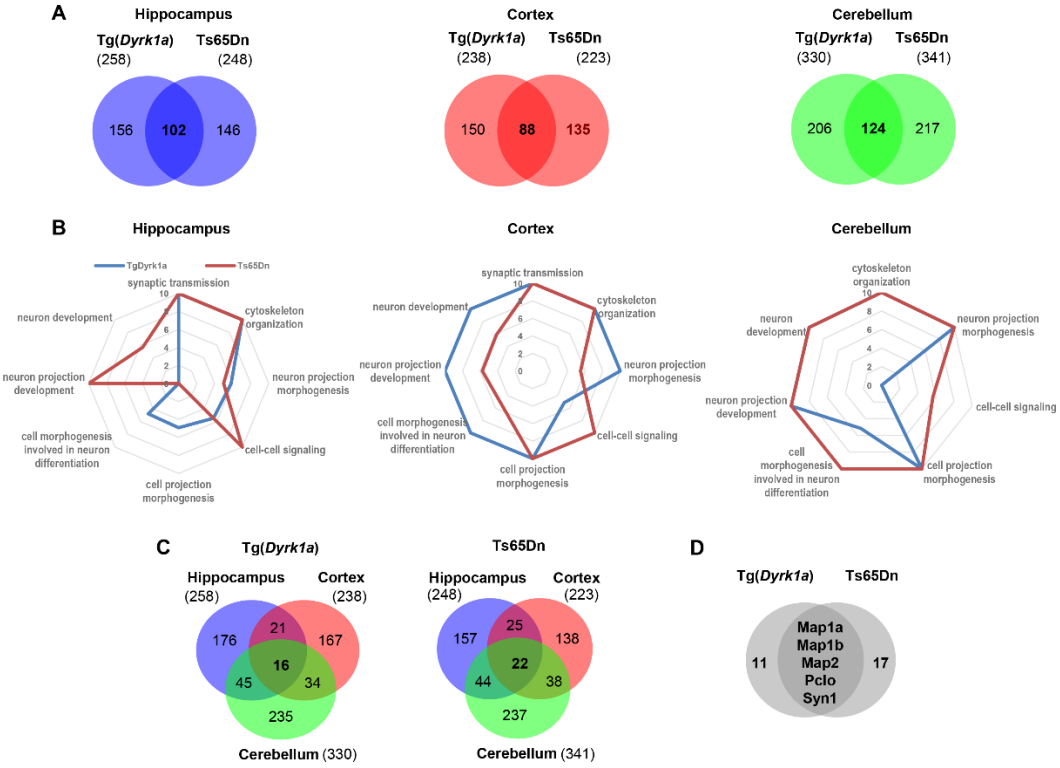

Figure 8. Phosphoproteomic analysis of Tg(*Dyrk1a*) and Ts65Dn mice brains following exposure to L41. Phosphoproteins, in each brain sub-structure, that are both up- or down-regulated by trisomy AND respectively down- and up-regulated by L41 treatment were selected for analysis. **A.** Venn diagrams comparing the two transgenic models vs. wt and vs. L41 treatment, at tissue level. 102, 88 and 124 modified phosphoproteins were common to the two models in hippocampus, cortex and cerebellum, respectively. Numbers in parentheses indicate dual modulated phosphoproteins in each model and each tissue. **B.** Biological processes enrichment deregulated by the phosphoproteins which are modulated one way in both Tg(*Dyrk1a*) and Ts65Dn mice and affected by L41 treatment in the opposite way. Represented here are those which are common to both models and to the three brain tissues. DAVID and ToppCluster analyses were performed respectively in hippocampus, cortex and cerebellum separately. Enriched classification is determined by the -log(P-value). Synaptic transmission, common to hippocampus and cortex, and cytoskeleton organization, common to the three brain regions, are the processes which are most modified by trisomy and sensitive to L41. **C**. Venn diagrams illustrate the number of dually modulated phosphoproteins in each model and in each tissue, and the numbers which are shared by different brain areas. 16 and 22 proteins were shared by all three tissues in Tg(*Dyrk1a*) and Ts65Dn mice, respectively. **D.** Venn diagram comparison of these 16 and 22 phosphoproteins revealed that 5 are shared by both models.

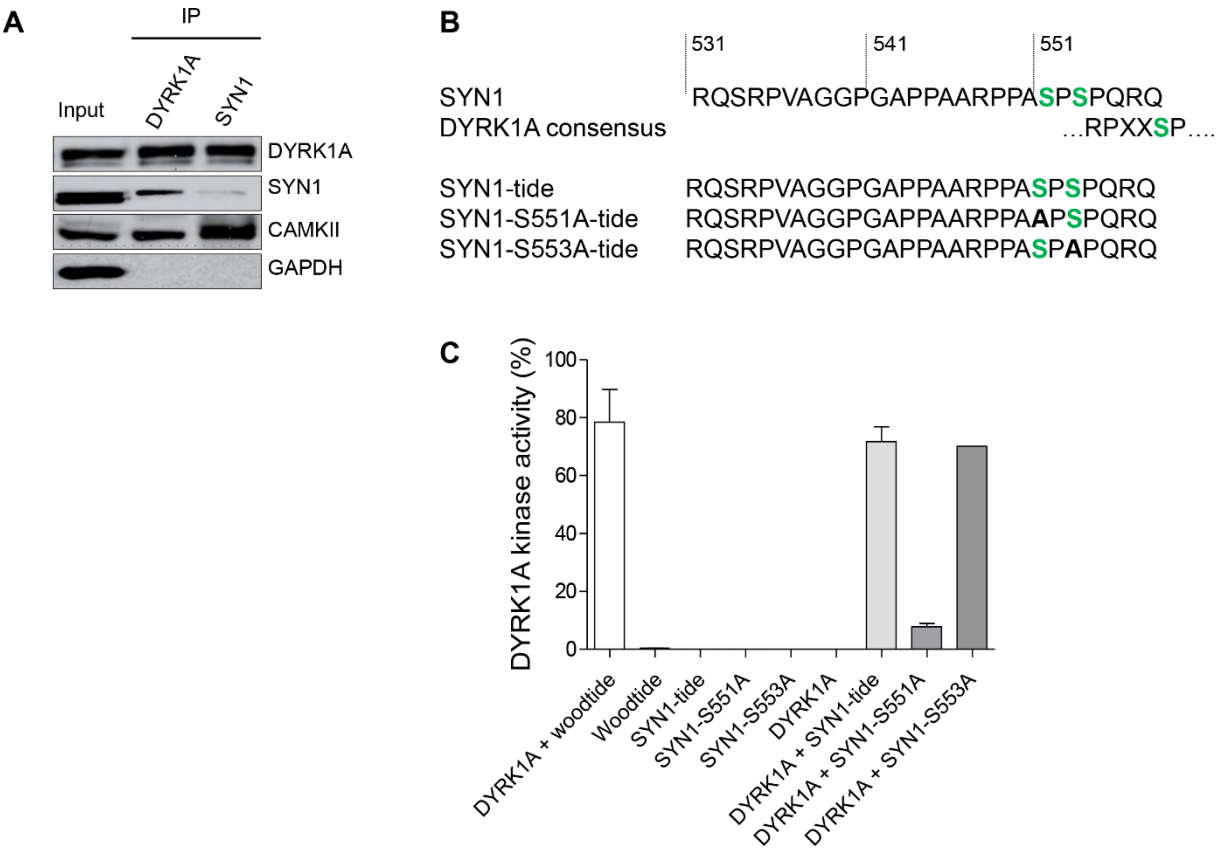

Figure 9. Direct interaction of DYRK1A and SYN1 (A, B), phosphorylation of SYN1 by DYRK1A (C, D). A. DYRK1A and SYN1 were immunoblotted following respective immunoprecipitation from wt mice brain extracts. DYRK1A or SYN1 present in the starting material (Input) are recovered in the IPs. SYN1 (74 kDa) is present in the DYRK1A IP and DYRK1A (85 kDa) is detected in the SYN1 IP, suggesting that these two proteins interact directly. Positive control of SYN1 IP was performed using an anti-CAMKII antibody. As expected, CAMKII (50 kDa) is present in the SYN1 IP. DYRK1A IP also brings down CAMKII, suggesting complexes between SYN1, CAMKII and DYRK1A. **B.** Sequence of SYN1 in the vicinity of Ser551 matches with the consensus DYRK1A phosphorylation site. Based on this sequence, 3 peptides were synthesized and used as potential substrates: SYN1, SYN1-S551A and SYN1-S553A. **C.** Kinase activity of recombinant DYRK1A towards the three different SYN1peptides. SYN1 and SYN1-S553A peptides were phosphorylated at the same level as Woodtide by recombinant DYRK1A (71.7% +/- 5.2%; 70.1% and 78.4% +/- 11.4% respectively). No significant catalytic activity was measured with the SYN1-S551A peptide (7.9% +/- 1.2%).

Sections	Word count (previous version)	Word count (new version)	Difference
Introduction	1405	1375	-30
Results	3152	3017	--135
Discussion	1982	1932	-50
Acknowledgment, Supplementary information, Authors contribution, Conflicts of interest	1930	1839	-91
Figure Legends	265	225	-39
TOTAL	**8734**	**8388**	**-346**

TABLE

Table 1. Summary of phosphoproteomic analyses

Model	Tg(*Dyrk1a*)			Ts65Dn			Common		
BRAIN AREA	**HIPP.**	**CORTEX**	**CEREB.**	**HIPP.**	**CORTEX**	**CEREB.**	**HIPP.**	**CORTEX**	**CEREB.**
Total protein number	886	948	1229	886	948	1229			
Total peptide number	1384	1523	2004	1384	1523	2004			
Modulated proteins, trisomic vs. wt	275	256	364	257	230	365			
Modulated peptides, trisomic vs. wt	333	296	437	311	270	422			
Modulated proteins, trisomic, L41 vs. vehicle	267	240	344	253	228	355	34	38	59
Modulated peptides trisomic, L41 vs. vehicle	321	275	403	307	265	410	40	38	63
phospho-Ser peptides	265	221	333	246	205	320	33	29	51
phospho-Thr peptides	39	44	58	53	42	75	6	6	11
phospho-Tyr peptides	17	10	12	8	18	15	1	3	1
phospho-Ser & phospho-Thr peptides	18	19	23	10	6	24			
phospho-Ser & phospho-Tyr peptides	5	1	4	2	3	4			
phospho-Thr & phospho-Tyr peptides	6	1	4	7	4	2			
DYRK1A phosphorylation sites	1	7	8	6	3	6			
Other kinases phosphorylation sites	279	251	383	263	223	351			